

Spectroscopic and mass spectrometric methods for the characterisation of metal clusters

Brian F.G. Johnson, J. Scott McIndoe *

Department of Chemistry, The University of Cambridge, Lensfield Road, Cambridge, CB2 1EW, UK

Received 13 September 1999; received in revised form 3 January 2000; accepted 26 January 2000

Contents

Abstract	902
1. Introduction	902
2. Spectroscopic techniques	902
2.1 Vibrational spectroscopy	902
2.2 NMR spectroscopy	904
2.3 UV–vis spectroscopy	906
2.4 Mössbauer effect spectroscopy	907
2.5 EXAFS spectroscopy	907
2.6 EPR spectroscopy	909
3. Mass spectrometric techniques	910
3.1 Electron impact ionisation	911
3.2 Inductively coupled plasma ionisation	913
3.3 Field desorption	913
3.4 Plasma desorption	914
3.5 Fast-atom bombardment	915
3.6 (Matrix assisted) laser desorption ionisation	917
3.7 Electrospray ionisation	920
4. Summary	927
Acknowledgements	928
References	928

* Corresponding author. Fax: +44-1223-336362.

E-mail address: jsm43@cam.ac.uk (J.S. McIndoe).

Abstract

This review covers some of the many spectroscopic and mass spectrometric techniques used to characterise transition metal clusters. Special attention has been paid to recent advances in mass spectrometry, which have allowed the study of compounds previously inaccessible to this method of characterisation. © 2000 Elsevier Science S.A. All rights reserved.

Keywords: Clusters; Characterisation; Spectroscopy; Mass Spectrometry.

1. Introduction

There are few areas of synthetic research which have been so dependent on the development of appropriate techniques of characterisation as cluster chemistry. The onset of high interest in metallic clusters came at a time when a range of new or modified techniques began to emerge. Dominant amongst these was more rapid crystal structure determination by X-ray diffraction, which furnished an effective means of structural analysis of highly complicated systems. Mass spectrometry was also applied successfully to the problem of cluster characterisation, and IR spectroscopy provided much useful information. These developments together with advances in multinuclear NMR aided the synthetic chemist to such an extent that they have become routine. Where appropriate, other spectroscopic techniques, such as EPR, EXAFS, Mössbauer and UV–vis spectroscopy, have also been utilised by the cluster chemist for the purposes of obtaining structural or kinetic data. Selected examples of the application of each of these spectroscopic techniques to the study of transition metal clusters are presented in this review.

The range of mass spectrometric methods now available to the cluster chemist is presented in more detail. Until moderately recent times mass spectrometric analysis was limited to those compounds which were neutral and highly volatile. This is no longer the case, and in this article we review the wide variety of ionisation methods now available and assess their usefulness in a wide range of charged and neutral cluster species.

2. Spectroscopic techniques

2.1. Vibrational spectroscopy

Infrared spectroscopy was one of the first instrumental techniques to be applied (being one of only a few available) to the study of transition metal carbonyl clusters. It is still a standard means of identifying carbonyl cluster compounds today, thanks to the speed and sensitivity of the technique. The CO stretching region typically exhibits strong bands in a region ($\sim 2150\text{--}1600\text{ cm}^{-1}$) largely free of absorptions from other functional groups, and samples may be conveniently

analysed as solutions. However, a characteristic of the vibrational spectra of carbonyl clusters is that they show many less bands than expected by group theory and therefore it is very difficult to draw firm conclusions about the structure or symmetry of the cluster based on IR evidence alone. An example of this spectral simplicity is shown in Fig. 1, the IR spectrum for $[\text{FeIr}_5(\text{CO})_{15}]^{3-}$.

The reasons for the simplicity of the IR spectrum has been a subject of debate and continues to draw interest [1]. For clusters, the fundamental question remains: when do the 'molecular surface selection rules' break down and the 'surface selection rules' take over? A recent analysis of a wide range of published transition metal cluster infrared spectra have led to the generalisation that most clusters can be treated by a spherical harmonic model that predicts a single peak in the terminal $\nu(\text{CO})$ region [2]. More detailed spectral analyses of clusters have also been carried out—qualitative arguments were used to obtain spectral assignment of the $\nu(\text{CO})$ vibrational (infrared and Raman) spectra of the cluster $\text{Ru}_3(\text{CO})_9(\mu_3\text{-}\eta^2\text{:}\eta^2\text{:}\eta^2\text{-C}_6\text{H}_6)$ [3], and confirmed by a normal coordinate analysis using the accurate force field available for $\text{Ru}_3(\text{CO})_{12}$ [4]. It has been suggested that the bridging spectral region is more structure-sensitive than the terminal region [5,6]. For example, the terminal $\nu(\text{CO})$ regions of the isostructural clusters $\text{Ir}_6(\text{CO})_{16}$, $[\text{FeIr}_5(\text{CO})_{16}]^-$ and $[\text{Fe}_2\text{Ir}_4(\text{CO})_{16}]^{2-}$ are very similar, yet their bridging $\nu(\text{CO})$ regions show considerable variation [7]. Some studies of the vibrational spectra of clusters have looked at other ligands, such as hydrides [8], interstitial atoms [9] or even the metal core [10],

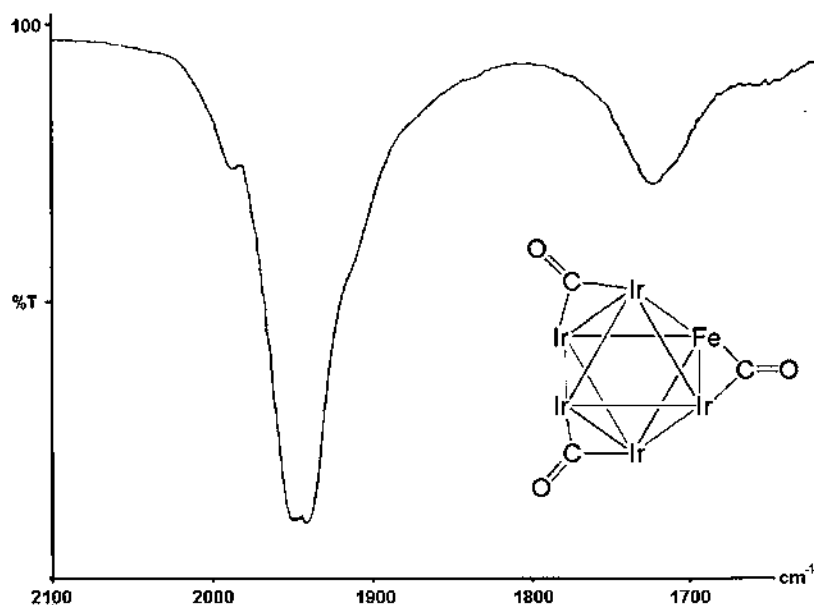


Fig. 1. The infrared spectrum (THF solution) of $[\text{FeIr}_5(\text{CO})_{15}]^{3-}$ (the diagram of the structure shows only the bridging COs (open circles); the terminal COs, two on each metal atom, are omitted for clarity. Reprinted with permission from Ref. [7].

but such investigations do not represent a routine means of characterisation. Infrared spectroelectrochemistry has been employed to study the reactivity of clusters, for example in examining the redox behaviour of $\text{Ru}_6\text{C}(\text{CO})_{17}$ and $[\text{NBu}_4]_2[\text{Ru}_6\text{C}(\text{CO})_{16}]$ [11].

An advance in IR spectroscopy with implications for cluster chemistry is the development of fibre-optic probes for in situ measurement of IR spectra during a reaction. This approach has been used to monitor reactions at elevated temperature [12] and inside electrochemical cells [13].

2.2. NMR spectroscopy

Modern nuclear magnetic resonance (NMR) spectroscopic techniques allow straightforward acquisition of spectra for many elements important in cluster chemistry including ^1H , ^{11}B , ^{13}C , ^{15}N , ^{19}F , ^{29}Si , ^{31}P , ^{103}Rh , ^{117}Sn and ^{195}Pt . Most other nuclei are more difficult to study, but with effort can yield useful spectra. NMR provides crucial insight into the nature of the coordination sphere of the metal, stereochemistry and metal–ligand bonding [14].

^1H - and ^{13}C -NMR spectroscopy was applied to organometallic clusters early on, and it was shown that they display a high degree of fluxionality [15,16]. The various coordination modes of carbonyl ligands on clusters can be differentiated using ^{13}C -NMR by virtue of their characteristic chemical shifts [17], the terminal ligand ^{13}C nucleus being more shielded [18]. Separate ^{13}C -NMR signals are observed for inequivalent CO ligands when the molecule is not fluxional on the NMR time scale. ^1H -NMR spectroscopy is most useful when studying clusters with hydride ligands, as their location can not always be pinpointed or even inferred from the X-ray crystal structure. For example, the presence of twelve hydrido atoms in the high-nuclearity cluster $\text{H}_{12}\text{Pd}_{28}(\text{PtPMe}_3)(\text{PtPPh}_3)_{12}(\text{CO})_{27}$ was revealed from the ^1H -NMR spectrum [19]. Terminal μ_2 and μ_3 -hydrides generally have high-field signals due to the fact they are heavily shielded — the range is typically $\delta - 8$ to $- 30$. Interstitial hydrides appear over an even greater range. Spin–spin coupling between other spin 1/2 nuclei such as ^{31}P , ^{103}Rh or ^{187}Os [20] can give spectra that enable the location of the hydride ligand on the cluster to be determined. Variable temperature NMR studies have proved to be very useful in studying the movement of hydrides and carbonyls around the metal core as well as for structural identification [21]. The mobility of ligands other than CO and H has also been examined. Fig. 2 shows the variable temperature ^1H -NMR spectrum of $\text{Os}_3(\text{CO})_8(\eta^2\text{-CH}_2\text{CH}_2)(\mu_3\text{-}\eta^2\text{:}\eta^2\text{:}\eta^2\text{-C}_6\text{H}_6)$, in which the alkene and benzene ligands were interpreted as undergoing ‘helicopter-like’ intramolecular rearrangements [22].

^{31}P -NMR spectroscopy is also extremely useful in cluster chemistry, as phosphorus ligands are commonplace. As well as assessing the number and type of ligands, coupling to NMR-active metal nuclei can provide further information on the environment of the phosphorus ligand. For example, the structure of the mixed-metal cluster $\text{Pt}_2\text{Rh}_2(\text{CO})_7(\text{PPh}_3)_3$ was established by the application of various multinuclear NMR techniques (^{13}C , ^{31}P , $\{^{31}\text{P}\text{--}^{31}\text{P}\}$ COSY and $\{^{13}\text{C}\text{--}^{103}\text{Rh}\}$ and $\{^{31}\text{P}\text{--}^{103}\text{Rh}\}$ heteronuclear multiple quantum coherence, HMQC) [23]. The metal

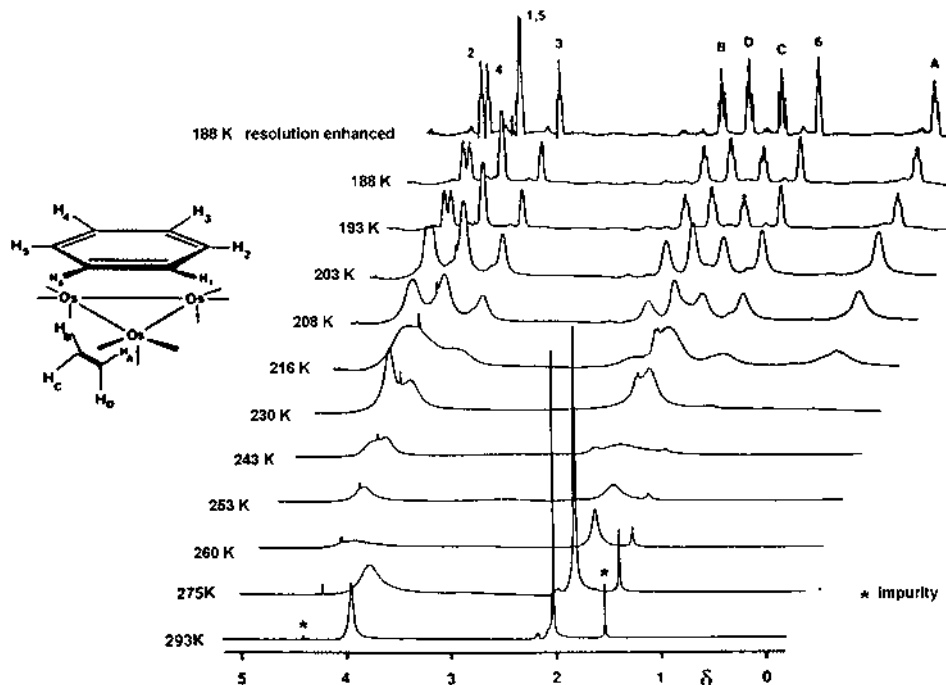


Fig. 2. The variable temperature ^1H -NMR spectrum of $\text{Os}_3(\text{CO})_8(\eta^2\text{-CH}_2\text{CH}_2)(\mu_3\text{-}\eta^2\text{:}\eta^2\text{:}\eta^2\text{-C}_6\text{H}_6)$. Reprinted with permission from Ref. [22]. Copyright 1992 American Chemical Society.

core of $[\text{Rh}_9\text{P}(\text{CO})_{21}]^{2-}$ was shown to be fluxional by ^{31}P -NMR, as the highly deshielded interstitial phosphorus atom produces a pattern that involves coupling of the phosphorus atom to nine equivalent rhodium atoms [24]. Upon cooling the pattern becomes more complex, indicating that the fluxionality has ceased on the time scale of the experiment.

Transition metal NMR spectroscopy has been used for some time to probe the metal core of clusters, with interesting results. For example, early studies of the ^{195}Pt -NMR spectra of $[\text{Pt}_n(\text{CO})_{2n}]^{2-}$ ($n = 3, 6, 9, 12, 15$) showed that not only do the Pt_3 triangles rotate with respect to one another at room temperature, interchange of Pt_3 triangles between clusters can also occur [25,26]. In recent years transition metal NMR spectroscopy has been boosted significantly by instrumental improvements, high-sensitivity detection methods and the availability of better databases of information on multinuclear NMR. While the very large chemical shift ranges of many transition metal nuclei can mean that finding the right signal is difficult, this property also means higher sensitivity to subtle structural perturbations. In addition to spin $\frac{1}{2}$ nuclei such as ^{57}Fe , ^{103}Rh and ^{187}Os , quadrupolar nuclei including ^{51}V , ^{53}Cr , ^{55}Mn , ^{59}Co and ^{91}Zr have also been studied [27]. Variable temperature multinuclear NMR has also been used successfully to probe the structure of transition metal carbonyl clusters [28].

The development of new NMR techniques has enabled the collection of high-resolution NMR spectra on solids [29]. One such technique is magic angle spinning (MAS), where the sample is spun at high speed at a particular angle with respect to the field axis. Compounds with ^1H , ^{13}C , ^{31}P and ^{29}Si and other nuclei have been studied in the solid state using this and other related techniques [30]. Examples of the utility of the technique include the examination of the solid state reactions of $\text{H}_2\text{Os}_3(\text{CO})_{10}$ with gaseous reactants (NH_3 , CO , H_2S) [31], studying the stereochemical non-rigidity of μ_3 -arene/olefin triosmium complexes in the solid state [32], the application of ^{31}P and ^{59}Co -NMR to the study of the structure and dynamics of the tetrahedral mixed-metal cluster $\text{HFeCo}_3(\text{CO})_9[\text{P}(\text{OCH}_3)_3]_3$ [33], or the location of hydride ligands on $(\text{NMe}_4)_{4-x}[\text{H}_x\text{Ni}_{12}(\text{CO})_{21}]$ ($x = 1, 2$) [34]. Solid-state NMR spectroscopy has provided evidence for the liberation of the Co_4 metal core inside the icosahedral carbonyl ligand shell of $\text{Co}_4(\text{CO})_{12}$ [35], in keeping with the ligand polyhedral model.

2.3. UV–vis spectroscopy

UV–vis data is only seldom collected for metal cluster compounds and even less often discussed, despite the fact that clusters are often very intensely coloured and give strong, distinctive UV–vis spectra. The structural information provided by the technique is limited, though intense colours can be indicative of high nuclearity clusters as the HOMO/LUMO gap is smaller than in low nuclearity clusters. UV–vis spectroscopy is most often used in cluster chemistry as a means of monitoring reactions to determine kinetics, such as following the substitution of CO ligands by PMe_3 on the tricobalt cluster $\text{Co}_3(\text{CO})_6[\mu_2\text{-}\eta^2\text{:}\eta^1\text{-C(Ph)C=C(PPh}_2\text{)C(O)OC(O)}](\mu_2\text{-PPh}_2)$ [36]. UV–vis spectroscopy is also useful in providing a match between species in solution and those absorbed onto a surface, for example the adsorption of $[\text{HRuOs}_3(\text{CO})_{13}]^-$ onto alumina [37], or the adsorption of clusters into zeolite pores [38]. UV–vis spectroelectrochemistry has been used to monitor structural changes in the high

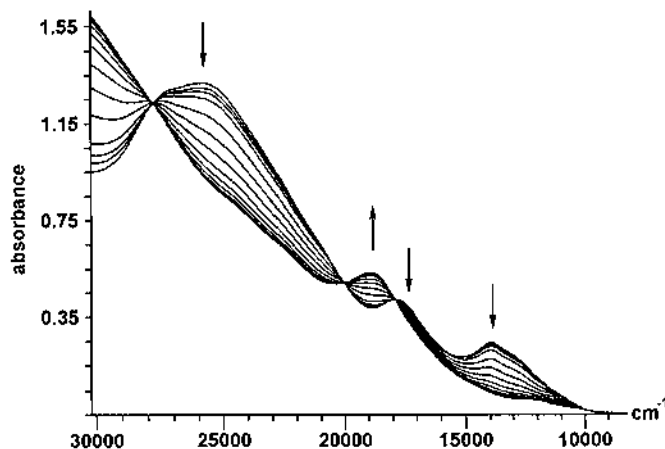


Fig. 3. The changes observed in the UV-Visible spectrum of $[\text{PPh}_4][\text{HRu}_{10}\text{C}(\text{CO})_{24}]$ upon exhaustive reduction. Reprinted with permission from Ref. [40].

nuclearity clusters $[\text{H}_x\text{Ru}_{10}\text{C}(\text{CO})_{24}]^{(2-x)-}$ ($x = 0, 1$) [39]. Fig. 3 shows the changes in the UV-Visible spectrum of $[\text{PPh}_4][\text{HRu}_{10}\text{C}(\text{CO})_{24}]$ upon exhaustive reduction.

In conjunction with voltammetric studies, the changes in the UV spectrum were interpreted as representing a significant structural change (CO elimination was disregarded as a possibility because the reaction was reversible), most likely the cleavage of an apical Ru–Ru bond.

2.4. Mössbauer effect spectroscopy

Mössbauer effect spectroscopy (MES) involves the nuclear resonance absorption (fluorescence) of γ -rays. In systems that contain Mössbauer atoms (~ 15 – 20 elements, for practical purposes) as central atoms, MES shows directly whether these atoms are situated in identical or different bonding states and environments [40]. This property was used to help show errors in the first X-ray structural examination of the cluster $\text{Fe}_3(\text{CO})_{12}$ by showing that the iron atoms were not in fact equivalent [41]. The technique is equally applicable to larger clusters and has been used to examine the (controversial) gold compound $\text{Au}_{55}(\text{PPh}_3)_{12}\text{Cl}_6$ to show that it has four unique gold atom environments (Fig. 4) [42].

MES can also be used to determine the site of substitution in heteropolynuclear compounds, such as showing that in the compounds $\text{FeCo}_2\text{S}(\text{CO})_{9-n}(\text{PPh}_3)_n$ ($n = 1, 2$) it is the cobalt atoms to which the phosphines coordinate preferentially [43]. The great advantage of MES is that amorphous samples can be studied. However, MES is necessarily limited to those clusters containing Mössbauer atoms and is not a routine technique largely for this reason. The technique is especially useful for iron clusters [44], as the ^{57}Fe nucleus is particularly sensitive. Tin and gold also possess suitable nuclei for study by MES.

2.5. EXAFS spectroscopy

Extended X-ray absorption fine structure (EXAFS) spectroscopy is an analytical technique, which provides structural information about molecules in any physical

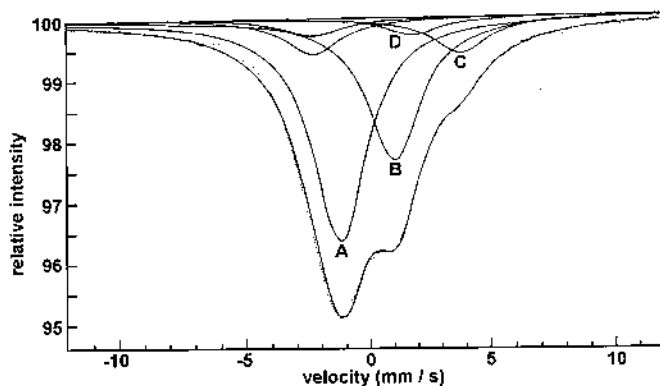


Fig. 4. The Mössbauer effect spectrum of $\text{Au}_{55}(\text{PPh}_3)_{12}\text{Cl}_6$. Reprinted with permission from Ref. [43].

state (including solutions and amorphous solids). Atoms absorb X-rays, and at a certain energy specific to each element an electron is ejected (ionisation). At this point an absorption edge appears in the EXAFS spectrum. The ejected electron travels out from the central absorbing atom, and back-scattering of this emitted electron wave off neighbouring atoms causes oscillations in the absorption coefficient near the edge. By analysing the frequency and amplitude of the oscillations, information about the local environment of the absorbing element can be derived. The primary limitations of EXAFS are the requirement for a synchrotron source for the X-radiation, and the fact that the information extracted from the EXAFS data is not easily converted into unambiguous three-dimensional structures.

The use of EXAFS for the characterisation of cluster species has been most popular for the study of catalytic materials generated by mounting clusters on various surfaces [45]. Clusters have been anchored inside zeolites [46], and the catalytic species is often formed by decarbonylation [47] or hydrogenation [48]. The assembly of large clusters from smaller precursors inside the zeolite has been carried out with success and is known as ‘ship-in-bottle’ synthesis [49]. EXAFS has been combined with XRD to investigate the effects of preparation conditions on the size of palladium clusters inside zeolite cavities [50]. Catalytic species have also been generated from cluster precursors on other surfaces, such as from $\text{PtRu}_5\text{C}(\text{CO})_{16}$ on carbon [51], $\text{Rh}_6(\text{CO})_{16}$ on a $\text{GeO}_2/\text{SiO}_2$ monolayer [52], $[\text{Pd}_6\text{Ru}_6(\text{CO})_{24}]^{2-}$ in mesoporous silica [53], or $\text{Ir}_4(\text{CO})_{12}$ on MgO powder [54], and been successfully studied using EXAFS.

Less frequently, EXAFS has been used to probe the structure of saturated clusters, and has shown, for example, the flexibility of the metal core in $[\text{Fe}_4\text{CoC}(\text{CO})_{14}]^-$ [55] and the non-rigidity of the metal core in $\text{Pd}_4(\text{CO})_4(\text{OAc})_4$ [56]. EXAFS may also be used to determine whether or not a structure persists in both solid state and solution. Such a study was carried out on $\text{Ru}_3\text{Pt}(\mu\text{-H})(\mu_3\text{-COMe})(\text{CO})_{10}(\text{PR}_3)$ ($\text{R} = \text{Cy}$, $i\text{Pr}$) [57], and small changes were ascribed to a more

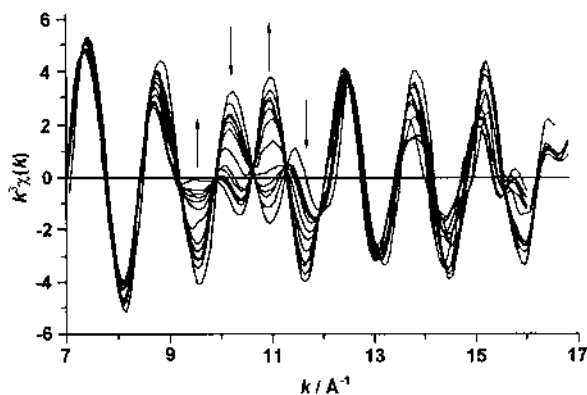


Fig. 5. The observed k^3 -weighted Pt L_{III} -edge EXAFS spectra for the rearrangement of $\text{Ru}_3\text{Pt}(\mu\text{-H})(\mu_4\text{-}\eta^2\text{-CC'Bu})(\text{CO})_9(\text{dppe})$ to $\text{Ru}_3\text{Pt}(\mu_4\text{-}\eta^2\text{-C}=\text{CH'Bu})(\text{CO})_9(\text{dppe})$ in THF solution. Measurements were made at intervals over a 12 h period. Arrows indicate the direction in which features developed. Reprinted with permission from Ref. [59].

symmetrical structure being present in solution in the absence of packing effects that distort metal-metal distances in the solid state. In a more detailed study, the rearrangement of the spiked triangular cluster $\text{Ru}_3\text{Pt}(\mu\text{-H})(\mu_4\text{-}\eta^2\text{-CC'Bu})(\text{CO})_9\text{(dppe)}$ in solution to the butterfly cluster $\text{Ru}_3\text{Pt}(\mu_4\text{-}\eta^2\text{-C}=\text{CH'Bu})(\text{CO})_9\text{(dppe)}$ was monitored over a period of 12 hours (Fig. 5) using EXAFS spectroscopy, to provide both structural and kinetic imaging of the reaction profile [58].

The reaction was shown to be first order, and the rate constant was determined as $6 \times 10^{-3} \text{ min}^{-1}$, a value comparable to that of $3.3 \times 10^{-3} \text{ min}^{-1}$ calculated from solution NMR studies [59].

2.6. EPR spectroscopy

Electron paramagnetic resonance (EPR, alternatively known as electron-spin resonance, ESR) spectroscopy is a complementary technique to NMR, enabling the study of paramagnetic compounds [60]. EPR measures the absorption of electromagnetic radiation by a paramagnetic system placed in a static magnetic field [61]. It can provide structural information on species in solution, in polycrystalline powders, and in single crystals. EPR gives information on the environment of the unpaired electron, and can help to decide the extent to which electrons are delocalised over the ligands.

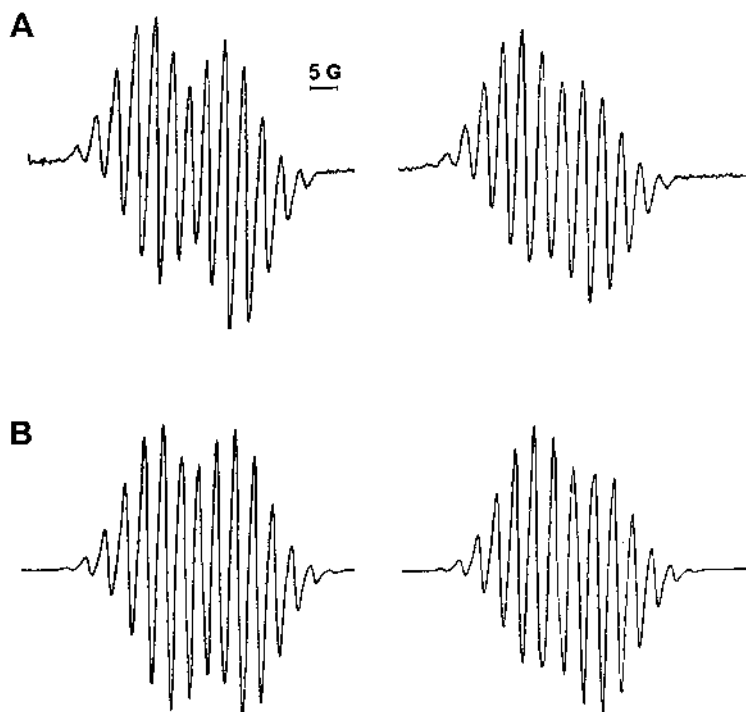


Fig. 6. Experimental (A) and simulated (B) EPR solution spectra of $[\text{NMe}_3\text{CH}_2\text{Ph}]_4[\text{Ag}_{13}\text{Fe}_8(\text{CO})_{32}]$. Reprinted with permission from Ref. [66]. Copyright 1992 American Chemical Society.

Iron–sulfur clusters often display paramagnetism and EPR is a popular means of studying such clusters, along with investigations of redox behaviour [62]. EPR measurements are frequently collected in conjunction with electrochemical studies [63]. Magnetic moment measurements and EPR have been used to identify unpaired electrons, such as in $[\text{Rh}_5\text{Ni}_6(\text{CO})_{21}\text{H}_x]^{3-}$; the odd electron was thought to necessitate the presence of either one or three hydrido atoms [64]. EPR can also be used to explain structural features. The EPR spectrum of the paramagnetic $[\text{Ag}_{13}\text{Fe}_8(\text{CO})_{32}]^{4-}$ tetra-anion in solution consists of two almost equally intense doublets, each split further into thirteen lines (Fig. 6(A)) [65].

The computer simulated spectrum matches perfectly (Fig. 6(B)), and the pattern indicates that the unpaired electron is strongly coupled to a central silver atom and loosely coupled to 12 peripheral silvers. This assignment was confirmed by the X-ray crystal structure, which showed a central Ag_{13} cuboctahedron. Overall, the cluster was suggested to have nine more electrons than that explained by most electron counting schemes. However, by considering the structure as an outer Fe_8 macrocube and an inner Ag_{12} cubeoctahedron encapsulating a neutral paramagnetic silver atom, the electron count is explicable [66].

3. Mass spectrometric techniques

The study of metal carbonyls by mass spectrometry has a long history. Thomson, the inventor of mass spectrometry [67], attempted to obtain a mass spectrum of $\text{Ni}(\text{CO})_4$ but the electric discharge he used to generate the ions caused the sample to decompose [68]. Later, Ni, Fe, Cr, Mo and W carbonyls were studied with excellent results (principally in efforts to determine the isotopic abundances of the metals). The first polynuclear metal carbonyl, $\text{Mn}_2(\text{CO})_{10}$, was examined by mass spectrometry over 50 years ago [69]. The highest mass ion observed was $\text{Mn}_2(\text{CO})_7^+$, but the authors pointed out (correctly) that the molecular weight may be greater as the parent-molecule ions are not always seen in a mass spectrum, remarkable since the electron counting methods familiar to us today were not known at that time.

Despite the development of cluster chemistry in the 1960s, study of polynuclear carbonyl clusters by mass spectrometry was not a routine technique. Instrument operators, used to dealing with organic compounds only, were often suspicious that decomposition of clusters in the machine would lead to their machines being damaged or ruined by metal deposits. However, these fears proved largely unfounded and early experiments on simple binary carbonyl clusters [70,71] were soon followed by studies of larger clusters [72]. Despite difficulties with carbonyl hydride clusters due to complications arising from the loss of both H and CO groups [73], mass spectrometry was shown to be a useful tool for elucidating the correct stoichiometry of such compounds (transition metals often possess a characteristic isotope pattern, which may be used to easily decipher the number of metals in an ion) [74]. An advantage in the study of neutral metal carbonyl clusters is their

reasonably high volatility. The high vacuum and raised temperature used in conventional mass spectrometry did not preclude the study of the more robust species. However, substituted, thermally sensitive and charged clusters, with or without carbonyl ligands, remained inaccessible to mass spectrometry due to lack of volatility or decomposition.

Analysis by mass spectrometry requires compounds to be in the gas phase, and the development of mass spectrometry is as much a story of generating gas-phase ions as it is of separating the ions by their mass-to-charge (m/z) ratio [75]. Many compounds cannot be vaporised without considerable, adverse decomposition, and these include the majority of cluster compounds. The techniques applied to volatile species are not always useful as they require stable, gas phase molecules. A great amount of effort was directed towards the problem of propelling involatile species into the gas phase and a number of solutions have been devised to extend the usefulness of mass spectrometry to the analysis of large, complex and fragile molecules.

3.1. *Electron impact ionisation*

Volatile compounds can be introduced into a mass spectrometer very easily, via inlets that allow the sample to 'leak' into the machine (these include the very well known gas chromatographic inlets). Compounds insufficiently volatile to be introduced by these methods can be inserted straight into the ion source using a direct probe inlet, passing through a vacuum lock. With heating and at high vacuum, good mass spectra of many relatively involatile compounds may be obtained. Once propelled into the gas phase, various means have been developed to ionise the neutral molecules to make them amenable to separation.

The classic ionisation technique is by means of electron impact (EI). Electrons are emitted from a resistively heated filament and accelerated through a voltage drop, typically 70 V. Because most covalent molecules have ionisation potentials of around 10 eV, an incident electron with a kinetic energy of 70 eV will dislodge an electron from one of the higher energy molecular orbitals. Molecular ions ($M^{+\bullet}$) are produced with varying internal energies, causing decomposition of those in higher energy states to break apart into fragment ions. Ionisation can also be achieved with high-energy photons in photo ionisation (PI), with electronically excited neutral species as in Penning ionisation (PeI), or with reactant gas ions as in chemical ionisation (CI) [76,77]. However, the utility of such sources for the mass spectrometry of cluster species is limited as they share the same limitation as EI in that the samples need to be volatile.

EI ionisation is quite effective for volatile clusters that are reasonably thermally stable, and has been used for some time. For example, excellent spectra of osmium clusters as large as $\text{Os}_8\text{C}(\text{CO})_{21}$ were obtained using EIMS some 25 years ago [78]. These spectra correctly identified the number of carbonyl ligands. For these large clusters elemental analysis and spectroscopic methods provided very little useful information, so the ability of mass spectrometry to establish the molecular formula

was crucial. Furthermore, mass spectrometry allowed the successful identification of interstitial carbide atoms.

The very low operating pressures of FTICR instruments (10^{-7} – 10^{-8} torr) [79] allow the study of even less volatile or thermally unstable compounds. For example, the molecular formulae of the triosmium methyldene clusters $\text{H}_3\text{Os}_3(\text{CO})_9(\text{CX})$ ($\text{X} = \text{Cl}, \text{Br}, \text{Ph}$) were established using EI-FTICR/MS, and the sequential loss of nine carbonyl groups further confirmed the assignment [80]. Likewise, useful mass spectra of the cluster $\text{H}_2\text{RhOs}_3(\text{CO})_{10}(\eta^5\text{-C}_5\text{H}_5)$ could not be obtained as a probe sample on a conventional instrument, because raising the probe temperature to give sufficient vapour pressure for the observation of high-mass peaks resulted in pyrolytic fragmentation [81]. However, the lower pressure of the FTICR instrument allowed excellent spectra of this compound to be obtained. The use of FTICR instruments also has the great advantage of extremely high resolution, providing unambiguous spectra of exceptional quality.

EI-FTICR mass spectrometry was used to unambiguously identify $\text{Pt}_4(\text{PF}_3)_8$ as the pyrolysis product generated from heating $\text{Pt}(\text{PF}_3)_4$ to temperatures below that required for metal deposition [82]. For this unusual cluster, NMR spectroscopy (^{19}F and ^{31}P) provided little information as the PF_3 groups were shown to be equivalent, but whether this feature was due to tetrahedral symmetry or to fluxional behaviour was unclear. No signal could be obtained using ^{195}Pt -NMR. Crystals failed to yield diffraction spots, and it was suggested that this may have been due to extensive motion of the molecule due to the fluorine atoms on the periphery. However, low-temperature studies also failed to resolve the problem.

Experiments using electron impact ionisation in conjunction with FTICR have been carried out to probe ion-molecule reactions of clusters. The ionised cluster is introduced to the ion chamber in the gas phase, in the presence of excess neutral

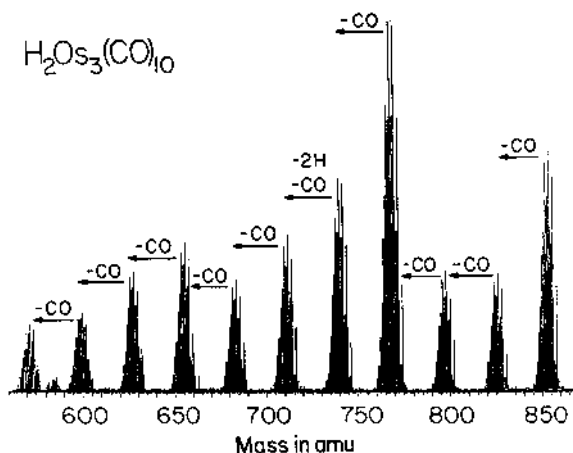


Fig. 7. The EI-FTICR mass spectrum of the parent ion region of $\text{H}_2\text{Os}_3(\text{CO})_{10}$. Reprinted with permission from Ref. [85]. Copyright 1988 American Chemical Society.

cluster. Because the ions may be trapped for a significant period of time (up to 10 s), ion–molecule reactions may be monitored. Cluster species as large as $[\text{Mn}_8(\text{CO})_{25}]^+$ from $\text{Mn}_2(\text{CO})_{10}$ and $[\text{Re}_3\text{Mn}_3(\text{CO})_{19}]^+$ from $\text{ReMn}(\text{CO})_{10}$ have been observed to form [83], and in similar experiments on $\text{H}_2\text{Os}_3(\text{CO})_{10}$, self-reaction via gas-phase ion–molecule reactions has been found to produce clusters containing up to 15 osmium atoms upon extended (≥ 0.5 s) trapping [84]. Fig. 7 shows the parent ion region of $\text{H}_2\text{Os}_3(\text{CO})_{10}$, and gives an indication of the excellent quality of the spectra that can be obtained using this technique

Negative-ion mode electron impact ionisation mass spectra of the clusters $\text{YCCo}_3(\text{CO})_9$ ($\text{Y} = \text{H}, \text{CH}_3, \text{C}_6\text{H}_5, \text{C}_6\text{H}_4\text{F}, \text{CO}_2\text{CH}_3, \text{F}, \text{Cl}$) have been obtained [85]. The molecular anions $[\text{YCCo}_3(\text{CO})_9]^-$ were found to be unstable and instead the fragment ions $[\text{YCCo}_3(\text{CO})_n]^-$ were observed, formed by electron capture and subsequent CO loss to form the fragment ions. The gas phase chemistry of these fragments was studied using FTICRMS, by allowing the anions to react with their neutral precursors. Higher-order clusters containing five or six cobalt atoms and both apical substituents, e.g. $[(\text{YC})_2\text{Co}_5(\text{CO})_{11}]^-$ or $[(\text{YC})_2\text{Co}_6(\text{CO})_{13}]^-$ were observed.

3.2. Inductively coupled plasma ionisation

For the purposes of elemental analysis, the inductively coupled plasma (ICP) source is useful but because it involves conversion of all analytes to singly charged gas-phase ions, it provides no chemical information regarding the molecular form or oxidation state of the element in the original sample [86]. Nonetheless, it can provide useful information on the ratios of various elements relative to others, and so the technique finds some use in studies of heteronuclear clusters. For example, ICP-MS analysis showed that the mixed-metal cluster $[\text{Pt}(\text{PPh}_3)(\text{AuPPh}_3)_6(\text{Cu}_4\text{Cl}_3\text{PPh}_3)](\text{NO}_3)$ had a Pt:Cu ratio of 1:5.9:4.0 [87]. Similarly, ICPMS provided a Pt:Cu ratio of 1:7.9:2.0 for the cluster $[\text{Pt}(\text{H})(\text{AuPPh}_3)_8(\text{CuCl})_2](\text{NO}_3)$ and a Pt:Cu:P ratio of 1:8.9:8.1 for $[\text{Pt}(\text{H})(\text{AuPy})(\text{AuPPh}_3)_8](\text{NO}_3)_2$ [88]. ICP analysis has also been applied to the heterometallic cluster $[\text{Mo}_6\text{BiS}_8(\text{H}_2\text{O})_{18}]^{8+}$, confirming the Mo:Bi:S ratio as 6:1:8 [89]. The clusters $[\text{Mo}_6\text{SnSe}_4(\text{H}_2\text{O})_{12}]^{6+}$ and $[\text{Mo}_6\text{SnSe}_8(\text{H}_2\text{O})_{18}]^{8+}$ were characterised in similar fashion [90]. The technique is a promising one for application to heteronuclear clusters for which single crystals can not be obtained.

3.3. Field desorption

Application of a high positive electric potential to an electrode in the shape of a point results in a very high potential gradient around the regions of high curvature. A molecule experiencing this field has its molecular orbitals distorted and quantum tunnelling of an electron can occur from the molecule to the positively charged anode. This process occurs in field ionisation (FI) [91]. The positive electrode (an array of very fine needles) repels the positive ion formed into the mass spectrometer. The practical consequence is that the molecular ion formed in this manner is

not excited, and very little fragmentation occurs, giving an abundant $[M]^+$ peak. The major drawbacks are that the high fields used generally require the use of a magnetic sector instrument and that anode preparation is tedious. Field desorption (FD) is closely related to FI, the major difference being that the sample is actually coated on the anode rather than being in the vapour phase around it. It suffers from the same drawbacks as FI, as well as being very sensitive to the temperature of the emitter, and its application to cluster chemistry has been limited. Nonetheless, a few clusters have been characterised using this method, such as the tetranuclear butterfly clusters $Ru_4(\mu-H)_2(CO)_8[R^1C=C(H)C(H)=NR^2]_2$ ($R^1, R^2 = Me, ^iPr; Me, Cy; Ph, ^iPr$) [92], or the linear cluster $FeRu_3(CO)_{10}[MeC=C(H)C(H)=N^iPr][PhC=C(H)C(H)=N^iPr]$ [93].

3.4. Plasma desorption

An assortment of ionisation techniques have been developed with a common idea, based on a proposal that sufficiently rapid heating could desorb or vaporise complex molecules before decomposition occurred, on the grounds of rate theory for unimolecular decomposition [94]. These ‘energy sudden’ methods rely on nearly instantaneous and large increases in temperature, generally achieved by particle bombardment of the sample. The first such technique to be developed was plasma desorption (PD), which uses radioactive ^{252}Cf as the particle source. This nucleus is radioactive and decomposes into two particles, each about half the nuclear mass, which travel with very high kinetic energies (millions of eV). One fission fragment passes through a thin film of sample, causing the sample to desorb directly as ions. The other particle is used to trigger a time-of-flight (TOF) mass analyser. Drawbacks are the low ion yield and the many hours required to obtain a spectrum, as well as the low resolution of the TOF analyser. Nonetheless, compounds with molecular masses in the tens of thousands have been successfully analysed.

The series of trinuclear nickel clusters $[Ni_3(\mu_3-L)(\mu_3-I)(\mu_2-dppm)_2]^{n+}$ ($L = I^-, CO, CNCH_3, CN-2,6-Me_2C_6H_3, CN^iC_3H_7, CN^iC_4H_9, CN^nC_4H_9$ and $NO^+, n = 0, 1, 2$) were characterised by PD and FABMS [95]. Strong molecular ion peaks were observed for all clusters except $L = NO^+$ for both techniques. Dimers of the trinuclear clusters, $\{[Ni_3(\mu_3-I)(\mu_2-dppm)_3]_2(\mu_3;\mu_3-\eta^1;\eta^1-CN-R-NC)\}^{2+}$ were prepared by the reaction of two equivalents of $L = I^-$ with one equivalent of the appropriate di-isocyanide, $CN-R-NC$ and unambiguously identified by PD and FAB.

Very different results were obtained from a study of high-nuclearity anionic platinum carbonyl clusters with Pt_{19} , Pt_{24} , Pt_{26} and Pt_{38} close-packed metal cores [96]. An envelope of peaks in the negative-ion spectrum corresponding to successive losses of CO from the intact metal core was observed. More extraordinary was the observation of a series of oligomeric ions formed from cluster aggregation, extending out beyond 100 000 m/z (in excess of 500 platinum atoms) in the case of the Pt_{26} cluster (Fig. 8) [97]. A similar but less abundant positive ion spectrum was also observed. The cation associated initially with the cluster was not incorporated into the oligomers.

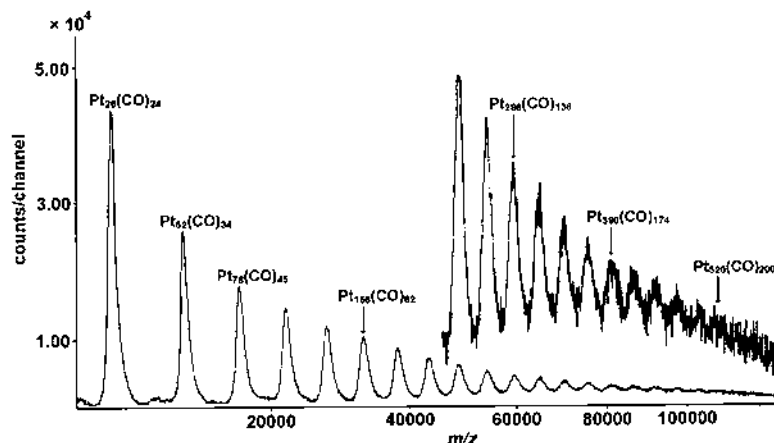


Fig. 8. The plasma desorption mass spectrum of $[\text{Pt}_{26}(\text{CO})_{32}]^{2-}$. Reprinted with permission from Ref. [98]. Copyright 1991 American Chemical Society.

PDMS has also been used to study the gold phosphine clusters $[\text{Au}_6(\text{PPh}_3)_6](\text{NO}_3)_2$, $[\text{Au}_6(\text{PPh}_3)_8](\text{NO}_3)_2$, $[\text{Au}_9(\text{PPh}_3)_8](\text{NO}_3)_3$, $[\text{Au}_{11}(\text{PPh}_3)_8\text{Cl}_2]\text{Cl}$, $\text{Au}_{13}(\text{PPh}_2\text{-Me})_8\text{I}_4$ and $[\text{CAu}_6(\text{PPh}_3)_6](\text{BF}_4)_2$, which had been previously well-characterised by other methods. Extensive fragmentation of these clusters occurred, to the extent that it was judged impossible to assign a structure or even a formula based on the mass spectral evidence [98]. The same authors [99] examined the large gold cluster first synthesised by Schmid and formulated as $\text{Au}_{55}(\text{PPh}_3)_{12}\text{Cl}_6$ [100], and despite being unable to prove or disprove this assignment (due to detecting only extremely broad ‘mass zones’ rather than discrete peaks), claimed that the synthesis of the compound was not entirely reproducible and that the product was likely to be inhomogeneous.

3.5. Fast-atom bombardment

FAB was developed in the 1980s [101]. A beam of fast-moving argon or xenon atoms is used to bombard the sample, which is dissolved in a non-volatile liquid such as glycerol and placed on the metal tip of a probe admitted to the ion source [102]. Momentum transfer causes ions of sample molecules to pass into the gas phase. Closely related to FAB is liquid secondary ion mass spectrometry (LSIMS), which uses fast ions (Ar^+ , Xe^+ , Cs^+) instead of atoms and is technically somewhat more convenient than FAB as it avoids the neutralising step. Molecular weights of up to 24 000 Da have been recorded. FAB can be complicated by redox, fragmentation and clustering processes in the study of metal complexes [103]. Nonetheless, FAB has become a relatively routine technique for mass spectrometric analysis of clusters, whether charged or neutral. Positive or negative ion spectra are produced with similar facility.

The positive ion FAB mass spectrum of $\text{Pt}_5(\text{CNC}_8\text{H}_9)_{10}$ shows a large number of peaks (see Fig. 9(a)) [104]. The highest mass peak, A, at $m/z = 2153$, is due to $[\text{M} - \text{CNC}_8\text{H}_9]^+$ and the most intense peak, I, is due to $[\text{M} - 7\text{CNC}_8\text{H}_9]^+$. The remaining peaks, labelled B to S in the figure, are readily assigned to losses of Pt

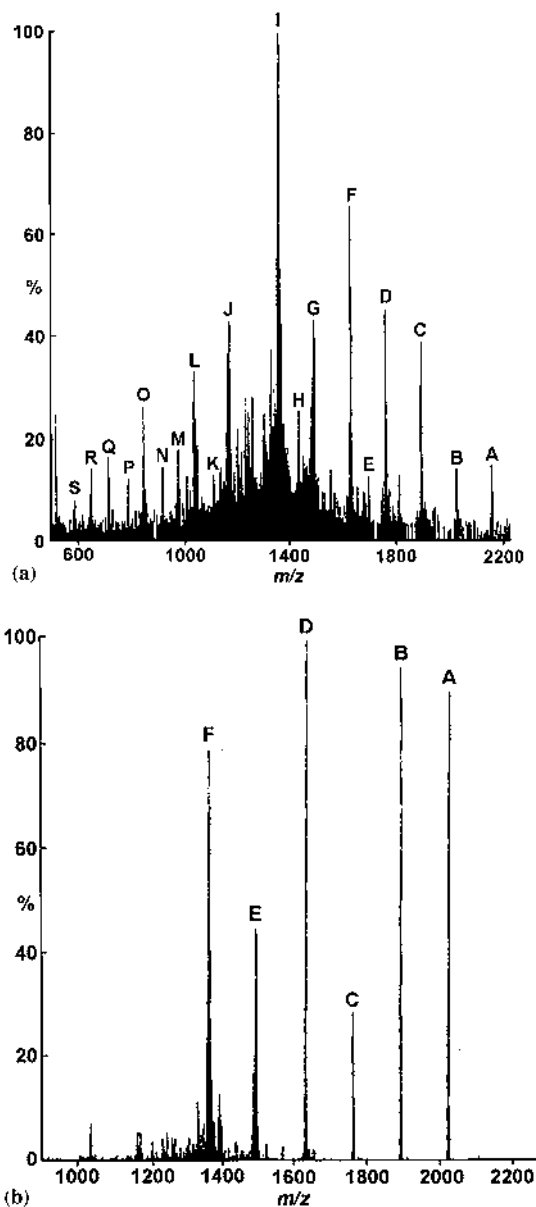


Fig. 9. The FAB mass spectra of (a) $\text{Pt}_5(\text{CNC}_8\text{H}_9)_{10}$ and (b) $\text{Pt}(\mu\text{-SO}_2)_2(\text{CNC}_8\text{H}_9)_8$. Reprinted with permission of The Royal Society of Chemistry from Ref. [105].

and/or CNC_8H_9 ligands. The spectrum of the related compound $\text{Pt}(\mu\text{-SO}_2)_2(\text{CNC}_8\text{H}_9)_8$ (see Fig. 9b) displays no sign of peaks retaining the SO_2 ligands, and $[\text{M} - 2\text{SO}_2]^+$ is the highest mass peak (A , $m/z = 2026$) with the remaining peaks due to losses of the CNC_8H_9 ligands $[\text{M} - 2\text{SO}_2 - x\text{CNC}_8\text{H}_9]^+$ ($x = 1-5$, B–F).

High-nuclearity clusters have been examined successfully using FABMS, such as the decanuclear clusters $[\text{Ru}_{10}\text{C}_2(\text{CO})_{22}(\text{L})]^2-$ and $[\text{Ru}_{10}\text{C}_2(\text{CO})_{23}(\text{L})]$ (L = diphenylacetylene or norbornadiene) [105], or the mixed-metal clusters $[\text{Re}_6\text{Ir}(\mu_6\text{-C})(\text{CO})_{20}(\text{AuPPh}_3)_{3-n}]^n-$ ($n = 1, 2, 3$) [106]. The large transition metal-gold clusters $[\text{Au}_2\text{Pt}(\text{PPh}_3)_4\text{NO}_3]\text{NO}_3$, $[\text{Au}_6\text{Pt}(\text{PPh}_3)_7](\text{BPh}_4)_2$, $[\text{Au}_2\text{Re}_2\text{H}_6(\text{PPh}_3)_6]\text{PF}_6$, $[\text{Au}_4\text{ReH}_4\text{-}\{\text{P}(p\text{-Tol})_3\}_2(\text{PPh}_3)_4]\text{PF}_6$ and other similar cationic and dicationic clusters were analysed by FAB [107], and gave well-resolved peaks for either the parent molecular ion $[\text{M}]^+$ for the cationic clusters or the ion pair $[\text{M} + \text{X}]^+$ (where X = counterion) for the dicationic clusters. Fragments were also observed, corresponding to losses of PPh_3 , H , CO , Ph and AuPPh_3 . A positive-ion FAB study of the cluster compounds $[\text{Au}_9\text{M}_4\text{Cl}_4(\text{PPh}_2\text{Me})_8][\text{C}_2\text{B}_9\text{H}_{12}]$ ($\text{M} = \text{Au}, \text{Ag}, \text{Cu}$) showed strong $[\text{M}]^+$ molecular ions as well as fragment peaks due to losses of primarily PPh_2Me but also of Au and Cl [108]. In another study, a range of high-nuclearity anionic ruthenium clusters were examined in negative-ion mode [109]. The anionic clusters gave intact anion peaks $[\text{M}]^-$, and all of the dianionic clusters gave protonated monoanions $[\text{M} + \text{H}]^-$ peaks. Degradation of the cluster metal frameworks of $[\text{HRu}_{10}\text{C}(\text{CO})_{24}]^-$ and $[\text{Ru}_{10}\text{C}(\text{CO})_{24}]^{2-}$ into $[\text{HRu}_6\text{C}(\text{CO})_{16}]^-$ was observed, and this degradation process parallels their reactivity in solution.

Halide clusters have also been characterised using FAB mass spectrometry. The clusters $[\text{Mo}_6\text{Br}_8\text{X}_6]^{2-}$ ($\text{X} = \text{CF}_3\text{CO}_2$, SCN , NCO , Cl , Br , I) gave negative-ion spectra in which the highest mass envelopes corresponded to the parent ion paired with one cation, the parent anion, and the parent anion minus one ligand [110].

3.6. (Matrix assisted) laser desorption ionisation

Laser desorption ionisation (LDI) achieves rapid heating by using a pulse of infrared radiation from an ultraviolet laser or similar, creating a gaseous plume containing positively and negatively charged ions. Time-of-flight (TOF) and Fourier transform ion cyclotron resonance (FTICR) mass analysers are well suited to these experiments because an entire spectrum can be generated with a single shot of the laser. When the sample is dispersed in a solid matrix (generally a compound that efficiently absorbs the laser radiation, such as nicotinic acid) the technique is termed matrix-assisted laser desorption ionisation (MALDI) [111], which has proved very popular for the study of polymers and large biomolecules [112]. The record molecular weight obtained for all types of compound is more than 1 000 000 Da [113]. Surprisingly, the application of MALDI to cluster compounds has been very limited (vide supra).

Aggregation processes that probably arise from ion–molecule reactions in the gas phase complicate the LDI spectra of neutral metal carbonyl clusters. The hexanuclear ruthenium carbide clusters $\text{Ru}_6\text{C}(\text{CO})_{17}$, $\text{Ru}_6\text{C}(\text{CO})_{14}(\eta^6\text{-C}_6\text{H}_5\text{Me})$, $\text{Ru}_6\text{C-}$

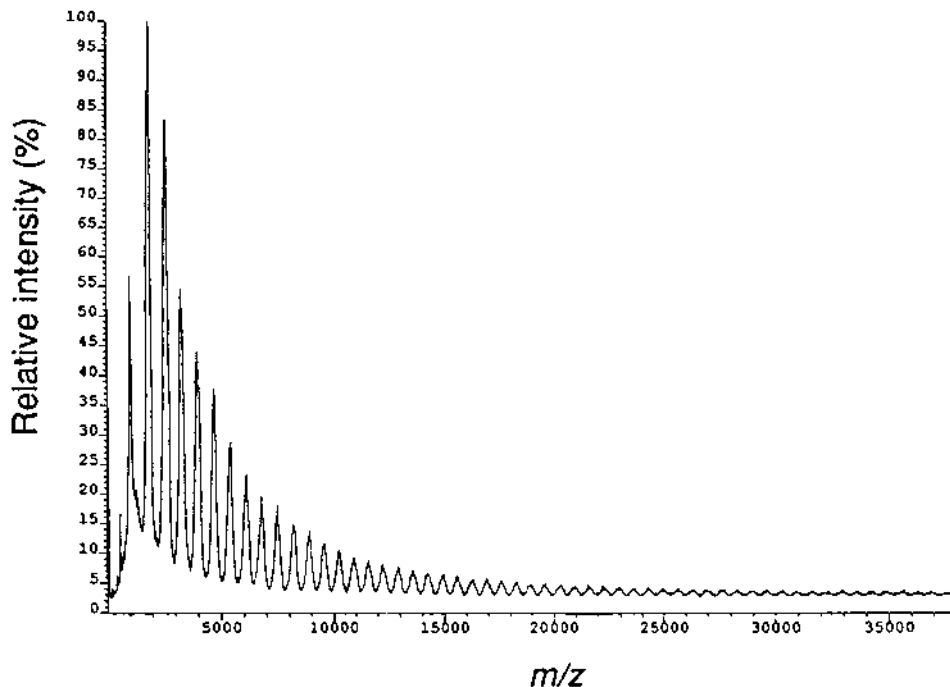


Fig. 10. The negative-ion LDI-TOF mass spectrum of $\text{Ru}_6\text{C}(\text{CO})_{17}$ in the range m/z 600–40 000. Reprinted with permission of The Royal Society of Chemistry from Ref. [116].

$(\text{CO})_{12}(\eta^6\text{-C}_6\text{H}_4\text{Me}_2)(\mu\text{-C}_6\text{H}_7\text{Me})$ and $\text{Ru}_6\text{C}(\text{CO})_{14}(\text{C}_{16}\text{H}_{16})$ all show high molecular weight clusters (up to 50,000 Da) formed by aggregation processes [114,115]. The negative-ion LDI-TOF mass spectrum of $\text{Ru}_6\text{C}(\text{CO})_{17}$ is shown in Fig. 10 and each peak represents a metal core, e.g. Ru_6 , Ru_{12} , Ru_{18} , Ru_{24} with varying numbers of CO ligands. For example, the peak at 3980 m/z contains the species $[\text{Ru}_{30}\text{C}_6(\text{CO})_x]^-$ ($x \sim 28\text{--}36$), but the width of each isotopomer envelope is such that considerable overlap occurs.

Fragmentation of the metal core further complicates the spectra of trinuclear clusters, and in a study of the clusters $\text{M}_3(\text{CO})_{12}$ ($\text{M} = \text{Fe}, \text{Ru}, \text{Os}$) species were observed in both positive and negative ion modes ranging in nuclearity from 1 to > 50 for $\text{Fe}_3(\text{CO})_{12}$, 2 to 9 for $\text{Ru}_3(\text{CO})_{12}$ and 3 to 11 for $\text{Os}_3(\text{CO})_{12}$ [116]. The negative-ion spectrum of $\text{Ru}_3(\text{CO})_{12}$ shows clearly fragmentation of the metal core, loss of CO ligands and aggregation processes (see Fig. 11).

Very similar processes of fragmentation and aggregation occur for the phosphine-substituted triruthenium clusters $\text{Ru}_3(\text{CO})_{12-x}(\text{PPh}_3)_x$ ($x = 1, 2, 3$) [117]. The phosphine ligands are stripped from the clusters during the desorption/ionisation process, and only homoleptic ruthenium carbonyl species $\text{Ru}_x(\text{CO})_y$ are observed in the mass spectrum.

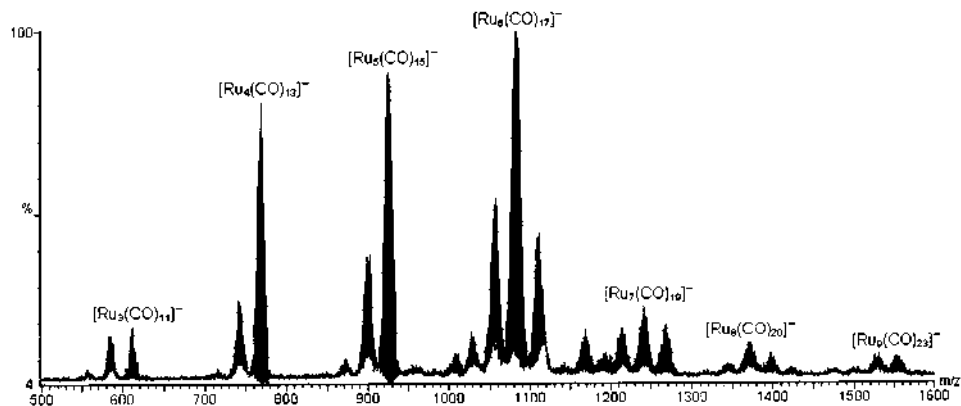


Fig. 11. The negative-ion LDI-TOF mass spectrum of $\text{Ru}_3(\text{CO})_{12}$. Reprinted with permission from Ref. [117]. Copyright 1999 American Chemical Society.

While the LDI mass spectra of neutral carbonyl clusters can be very complicated, LDI has been shown to be a useful method for the characterisation of large anionic osmium clusters [118]. The spectra obtained are clean and uncomplicated by aggregation, and the only fragment ions present are due to CO loss. Fig. 12 shows the LDI-TOF spectrum of $[\text{Os}_{10}\text{C}(\text{CO})_{24}]^{2-}$, which contains peak envelopes for the ions $[\text{Os}_{10}\text{C}(\text{CO})_x]^-$ ($x = 7-24$).

The phosphorus containing clusters $\text{Fe}_4(\eta^5\text{-C}_5\text{H}_4\text{Me})_4(\text{CO})_6\text{P}_8$ and $\text{Fe}_6(\eta^5\text{-C}_5\text{H}_4\text{Me})_4(\text{CO})_{13}\text{P}_8$ have been successfully characterised by LDI-FTICR mass spectrometry [119]. A comparative analysis of LDI-FTICR and EI-FTICR mass spectra of four organometallic complexes of varying volatilities, including the dimers $\text{Fe}_2(\eta\text{-C}_5\text{Me}_5)_2(\mu\text{-P}_2)_2$ and $\text{Co}_2(\eta\text{-C}_5\text{Me}_5)_2(\mu\text{-P}_2)_2$, concluded that LDI gave either similar or much superior information to that provided (if at all) by EI, especially when the target complex was thermally unstable [120]. The halide clusters

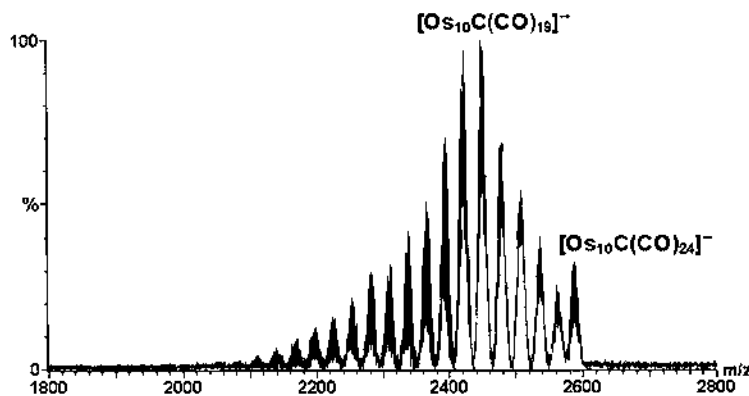


Fig. 12. The negative-ion LDI-TOF mass spectrum of $[\text{PPN}]_2[\text{Os}_{10}\text{C}(\text{CO})_{24}]$.

$[(\text{Nb}_6\text{X}_{12})\text{X}_2(\text{H}_2\text{O})_4]\cdot 4\text{H}_2\text{O}$ ($\text{X} = \text{Cl}, \text{Br}$) were studied using LDI-FTICR mass spectrometry [121]. The quasi-molecular ion $[(\text{Nb}_6\text{X}_{12})\text{X}_2]^-$ and fragment ions involving losses of 1–3 X were the most abundant in the spectrum, indicating the stability of the core cluster, Nb_6X_{12} .

The first example of the application of MALDI to cluster chemistry came recently in a study of the clusters $\text{Cs}_3\text{Re}_3\text{X}_{12}$ ($\text{X} = \text{Cl}, \text{Br}$) and $(\text{NBu}_4)_2[\text{Re}_2\text{Cl}_8]$. The clusters were examined using LDI with and without the use of a matrix [122]. MALDI produced the best spectra, and characteristic fragments due to loss of X gave peaks that were used to identify the number of rhenium atoms and the identity of the ligands, by the isotope patterns and m/z values. The same authors have since successfully extended the utility of the technique to the cluster anions $[\text{Re}_3(\mu_3\text{-E})(\mu\text{-Cl})_3\text{Cl}_6]^{2-}$ ($\text{E} = \text{S}, \text{Se}, \text{Te}$) [123]. MALDI has also been used to characterise a number of different dendritic carbosilanes containing ethynyl groups and dicobalt hexacarbonyl clusters on the periphery [124]. Molecular masses of up to 8500 Da have been successfully established [125].

Laser ablation has been used for the generation of metal cluster species. For example, laser ablation of CoS yields 83 gaseous ions $[\text{Co}_x\text{S}_y]^-$, detected and characterised by FTICR mass spectrometry [126]. The ions range in size from $[\text{CoS}_2]^-$ to $[\text{Co}_{38}\text{S}_{24}]^-$. Similar experiments have been carried out with FeS, NiS [127] and MnS [128]. Many experiments have also been carried out with various metal cluster sources attached to mass spectrometers, but are beyond the scope of this review, which is focused primarily on the characterisation of preformed clusters.

3.7. Electrospray ionisation

Electrospray ionisation (ESI) involves spraying a solution of a substance through a capillary into a chamber, through which is passing a stream of dry gas in the opposite direction to the spray [129]. A potential of several kilovolts is applied between the capillary and the chamber wall. Charged droplets are produced that become smaller as the solvent is evaporated, and eventually bare ions are formed which pass through a glass capillary into the pre-analyser region, where the remaining bath gas and residual solvent is pumped away. The ions are then focused through the lensing system into the analyser of the mass spectrometer. Electrospray mass spectrometry experiments were first carried out by Dole and colleagues some 30 years ago [130]. However, the real birth of ESIMS as an analytical tool came in the mid-1980s when Fenn and co-workers improved on Dole's designs and coupled an electrospray source to a quadrupole mass analyser [131]. Once it was shown that ESIMS could provide accurate molecular weights (with seemingly no upper limit) for proteins and other large, fragile molecules [132,133] it led to an explosion of interest in the technique, which has continued unabated.

Ionic compounds are particularly well suited to study by electrospray mass spectrometry. They are transported into the gas phase essentially without change and spectra typically consist of a single envelope of peaks due to the intact ion, with little or no fragmentation. Ionic inorganic species, quaternary ammonium and

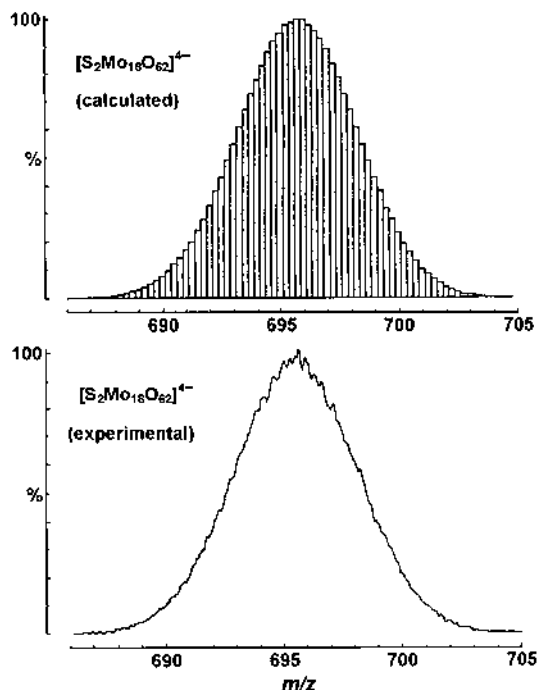


Fig. 13. Comparison of calculated and experimental negative-ion ESI mass spectral isotope pattern for $[\text{S}_2\text{Mo}_{18}\text{O}_{62}]^{4-}$.

phosphonium salts, were amongst the very first compounds to be studied by ESIMS [134]. Inorganic chemists quickly realised the potential of the technique [135]. A study by Chait in 1990 showed that electrospray ionisation generated intact principal ions for ruthenium(II) dipyriddy complexes [136]. Anionic clusters were soon being examined using ESIMS, with a notable early example being the successful characterisation of the quadruply-charged heteropolymolybdate $[\text{S}_2\text{Mo}_{18}\text{O}_{62}]^{4-}$ [137]. Fig. 13 shows the comparison between the experimental and expected mass distribution patterns for this ion. The polymerisation of $[\text{MoO}_4]^{2-}$ that occurs upon acidification has been studied [138], with a number of new isopolyoxomolybdate species being identified. The formulation and speciation of these products has been difficult to establish by other methods.

Organometallic complexes can also provide good electrospray spectra [139]. The mixed metal anionic clusters $[\text{Fe}_3(\text{CO})_{11}(\mu\text{-HgX})]^-$ [$\text{X} = \text{Co}(\text{CO})_4$, $\text{Mn}(\text{CO})_5$, $\text{Fe}(\text{CO})_2\text{Cp}$, $\text{W}(\text{CO})_3\text{Cp}$ and $\text{Mo}(\text{CO})_3\text{Cp}$] and $[\text{Fe}_6\text{C}(\text{CO})_{16}(\text{AuPPh}_3)]^-$ gave good negative-ion spectra with either the $[\text{M}]^-$ or the $[\text{M} - \text{CO}]^-$ peak being the most intense in the spectrum [140]. The related clusters $[\text{Fe}_4\text{C}(\text{CO})_{12}(\mu\text{-HgX})]^-$ ($\text{X} =$ as before) gave $[\text{M}]^-$ as the base peak in the spectrum [141]. Larger clusters also provide excellent quality spectra, such as for the dianionic clusters $[\text{Ni}_{10}(\text{BiMe})_2(\text{CO})_{18}]^{2-}$ [142], $[\text{Ru}_6\text{C}(\text{CO})_{16}]^{2-}$ and $[\text{Os}_{10}\text{C}(\text{CO})_{24}]^{2-}$ [143]. A spec-

trum of $[\text{Os}_{10}\text{C}(\text{CO})_{24}]^{2-}$ is presented in Fig. 14 that displays the lack of fragmentation typical of ESIMS.

Clusters in which the charge resides on the ligand, such as the water-soluble cluster $\text{Ru}_3(\text{CO})_9[\text{P}(\text{C}_6\text{H}_4\text{SO}_3\text{Na})_3]_3$, can provide good negative-ion spectra [144]. Cationic clusters have also been investigated successfully, such as the water-soluble tetraosmium cluster $[\text{Os}_4(\mu\text{-H})_4(\text{CO})_{10}(\text{dppH})]^+$ (dpp = 2,3-bis(2-pyridyl)pyrazine) [145]. ESIMS has been used to study the constitution of mercury and mixed mercury/cadmium dithiocarbamate cations in dichloromethane and methanol solutions [146]. Average empirical compositions had been previously established by chemical, electrochemical and NMR techniques, but all showed evidence of lability between several species in solution. ESIMS was shown to be well suited to studying labile, charged polynuclear species in solution and a large number of ionic oligomers were successfully identified.

ESIMS promises to be a very useful technique for the monitoring of cluster reactions. Experiments can be done on a very small scale varying the reaction conditions and times, enabling rapid and inexpensive optimisation. Furthermore, monitoring by ESIMS can in certain cases be useful in identifying intermediates and minor products, and in this case ESIMS is superior to IR spectroscopy as the latter technique often suffers from overlap of bands from different species. Recent success has been had with this approach in the study of the reaction between $\text{GeCo}_4(\text{CO})_{14}$ and $[\text{Co}(\text{CO})_4]^-$. This reaction was first studied in 1982 and the product, $[\text{GeCo}_5(\text{CO})_{16}]^-$, was characterised by X-ray crystallography and IR spectroscopy [147]. Re-examination of this reaction in ether and CH_2Cl_2 and monitoring its course by ESIMS showed both this product as well as $[\text{GeCo}_7(\text{CO})_{20}]^-$ and $[\text{Ge}_2\text{Co}_7(\text{CO})_{21}]^-$, previously made from reactions of $[\text{GeCo}_5(\text{CO})_{16}]^-$ [148]. Furthermore, a new product, the previously unknown dianion $[\text{Ge}_2\text{Co}_{10}(\text{CO})_{24}]^{2-}$ (see Fig. 15) was also identified. The disappearance of the $[\text{Co}(\text{CO})_4]^-$ starting material was also demonstrated [149].

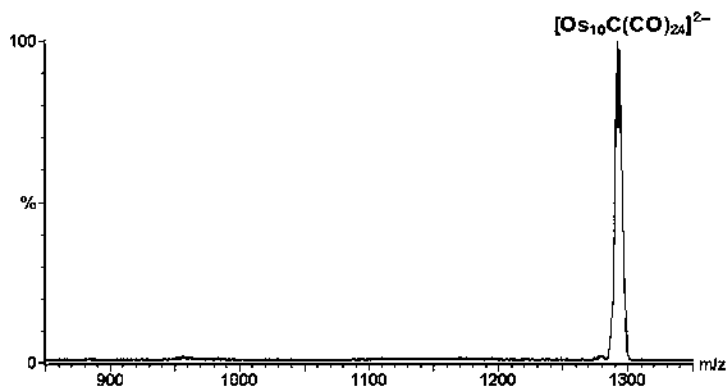


Fig. 14. The negative-ion ESI mass spectrum of $[\text{PPN}]_2[\text{Os}_{10}\text{C}(\text{CO})_{24}]$ run in a methanol mobile phase at low (15 V) cone voltage.

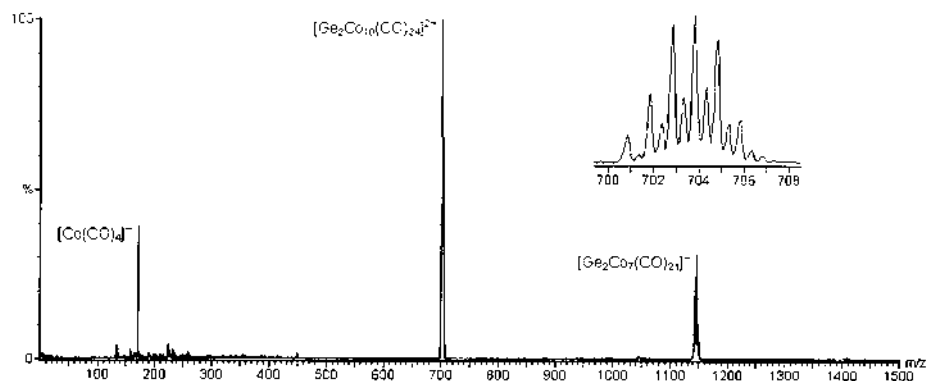


Fig. 15. The negative-ion ESI mass spectrum recorded during the reaction between $\text{GeCo}_4(\text{CO})_{14}$ and $[\text{Co}(\text{CO})_4]^-$ (see Ref. [150]).

By performing the reaction at the optimum temperature and stopping it after the yield of $[\text{Ge}_2\text{Co}_{10}(\text{CO})_{24}]^{2-}$ was shown to be highest, this new compound was successfully isolated and structurally characterised. The structure of the dianion, shown in Fig. 16, is highly unusual and could certainly not have been predicted from the mass spectrometric evidence alone.

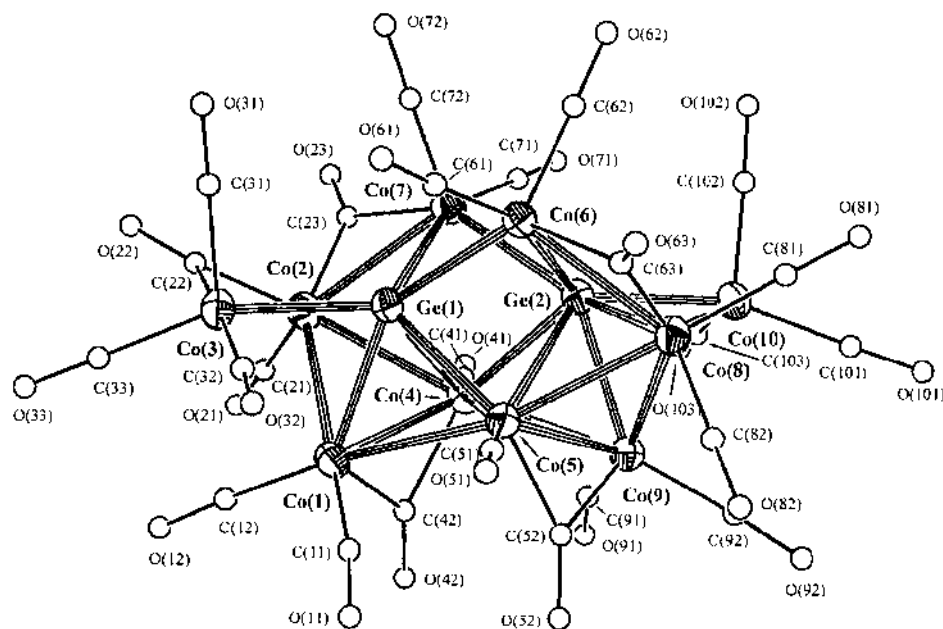
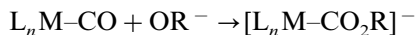


Fig. 16. The structure of $[\text{Ge}_2\text{Co}_{10}(\text{CO})_{24}]^{2-}$ (see Ref. [150]).

Much cluster synthesis involves the use of an inert atmosphere. Sampling reactions using a syringe and injecting the (usually further diluted) solution directly into the ionisation source is generally sufficient to exclude air or moisture, but interfacing a Schlenk line with the mass spectrometer is also possible and offers a versatile solution to the problem of air-sensitivity [150].

A number of methods have been developed for the analysis of neutral metal carbonyl clusters using ESIMS [115]. Because the oxygen of the carbonyl ligand is not appreciably basic, it will not protonate and hence species of the type $[M + H]^+$ are not observed. Various other charged species have, however, been shown to derivatise neutral carbonyl clusters. The most effective and general method to date is the use of alkoxide ion as an ionisation agent [151]. The sample is dissolved in the corresponding alcohol, and a small quantity of sodium alkoxide solution is added. Nucleophilic attack by the alkoxide ion on a coordinated carbonyl ligand provides a charged species:



This reaction is quite general for metal carbonyl compounds, is rapid and large equilibrium constants favour the product, all of which are ideal characteristics for a derivatisation process. Table 1 shows a representative range of carbonyl clusters that has been successfully analysed using this technique.

Metal carbonyl clusters, $M_x(CO)_y$, are also attacked by the nucleophilic azide ion, N_3^- , to form isocyanato complexes of the type $[M_x(NCO)(CO)_{y-1}]^-$. This reaction has been studied by ESIMS and the isocyanato complexes observed for the clusters $M_2(CO)_{10}$ ($M = Mn, Re$), $M_3(CO)_{12}$ ($M = Ru, Os$) and $Ir_4(CO)_{12}$ [152]. The azide-addition complex $[M_x(CO)_y + N_3]^-$ was also observed for some clusters, the first time evidence for this intermediate has been obtained. ESIMS appears to be an ideal means of screening substrates to see which are most suitable for subsequent small-scale reactions.

Silver (I) ions also work as ionisation agents with some neutral metal carbonyl clusters, such as $Ru_3(CO)_{12}$, $Os_3(CO)_{12}$, $Re_2(CO)_{10}$ and $SiFe_4(CO)_{16}$, providing $[M + Ag]^+$ and/or $[M + Ag + solvent]^+$ type ions (depending on the solvent and the cone voltage) [153]. It seems likely that the interaction is between an electron-rich metal-metal bond of a cluster and the silver ion to form a M_2Ag triangle [144]. Clusters of this type are known which are sufficiently stable to be characterised structurally, though all the examples have strongly electron donating ligands.

Table 1

Examples of neutral metal carbonyl clusters that give clean $[M + OMe]^-$ ions upon derivatisation with NaOMe

$Mn_2(CO)_{10}$	$Fe_3(CO)_{11}(CN^tBu)$	$Rh_4(CO)_{12}$	$Ru_6C(CO)_{17}$
$Re_2(CO)_{10}$	$Ru_3(CO)_{12}$	$Ir_4(CO)_{12}$	$Rh_6(CO)_{16}$
$[Fe(CO)_2Cp]_2$	$Os_3(CO)_{12}$	$NiRu_3(\mu-H)_3(CO)_9$	$Ru_6C(CO)_{14}(\mu_3-\eta^6-C_{16}H_{16})$
$[Mo(CO)_3Cp]_2$	$Ru_3(CO)_{11}PPh_3$	$Ru_4H_4(CO)_{12}$	$Ru_6C(CO)_{14}(\eta^6-C_6H_5Me)$

Further evidence for this form of association is given by the fact that Ag^+ does not give $[\text{M} + \text{Ag}]^+$ ions with mononuclear compounds.

The alkali metal ions Li^+ , Na^+ and K^+ will also associate with very electron-rich clusters such as $\text{Ru}_3(\text{CO})_9(\text{PPh}_3)_3$ to give species of the type $[\text{M} + \text{cation}]^+$. Because this ionisation method works equally well with the mononuclear carbonyl complexes *fac*- $[\text{Re}(\text{X}_2\text{bipy})(\text{CO})_3\text{Y}]$ (X_2bipy = 4,4'- X_2 -2,2'-bipyridine; X = H, Me, CF_3 ; Y = CN, Cl, Br, OCHO) [154] or the nitrosyl complexes $[\text{Ru}(\text{NO})\text{Cl}_3(\text{EPh}_3)_2]$ (E = P, As, Sb) [155], it seems that the alkali metal cations are associating in a different way to the silver ions. The attachment is likely to be via an *iso*-carbonyl (or *iso*-nitrosyl) link of the type $\text{L}_n\text{M}-\text{C}\equiv\text{O}\cdots\text{Na}^+$.

Another strategy for obtaining electrospray mass spectra from neutral clusters is by use of 'electrospray-friendly' ligands, namely phosphines bearing basic groups that can be readily protonated under electrospray conditions [156]. Derivatives of triphenylphosphine, $\text{PPh}_n(p\text{-C}_6\text{H}_4\text{OMe})_{3-n}$ and $\text{PPh}_n(p\text{-C}_6\text{H}_4\text{NMe}_2)_{3-n}$ (n = 0, 1, 2), have been shown to provide good positive ion electrospray spectra when bound to triruthenium clusters, and have the advantage that they are both chemically and electronically similar to PPh_3 .

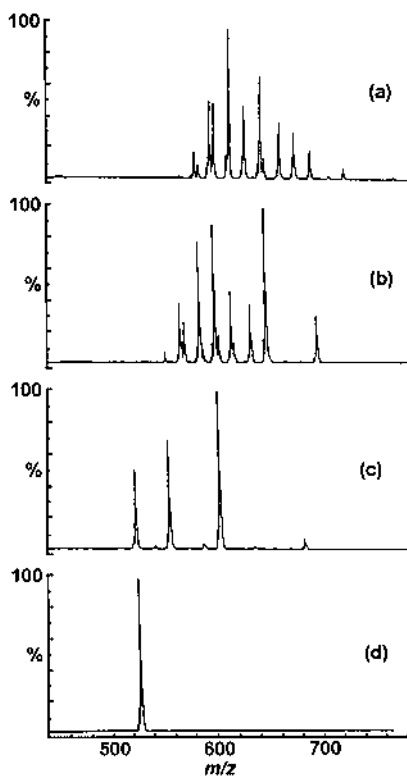


Fig. 17. ESI mass spectra at different ion source voltages of $[\text{Cr}_3\text{O}(\text{CH}_3\text{COO})_6(\text{H}_2\text{O})_3]^+$ dissolved in pyridine (2 mM) and diluted (1:10) with methanol: (a) 30 V; (b) 40 V; (c) 60 V; (d) 100 V. Reprinted with permission from Ref. [160]. Copyright 1993 American Chemical Society.

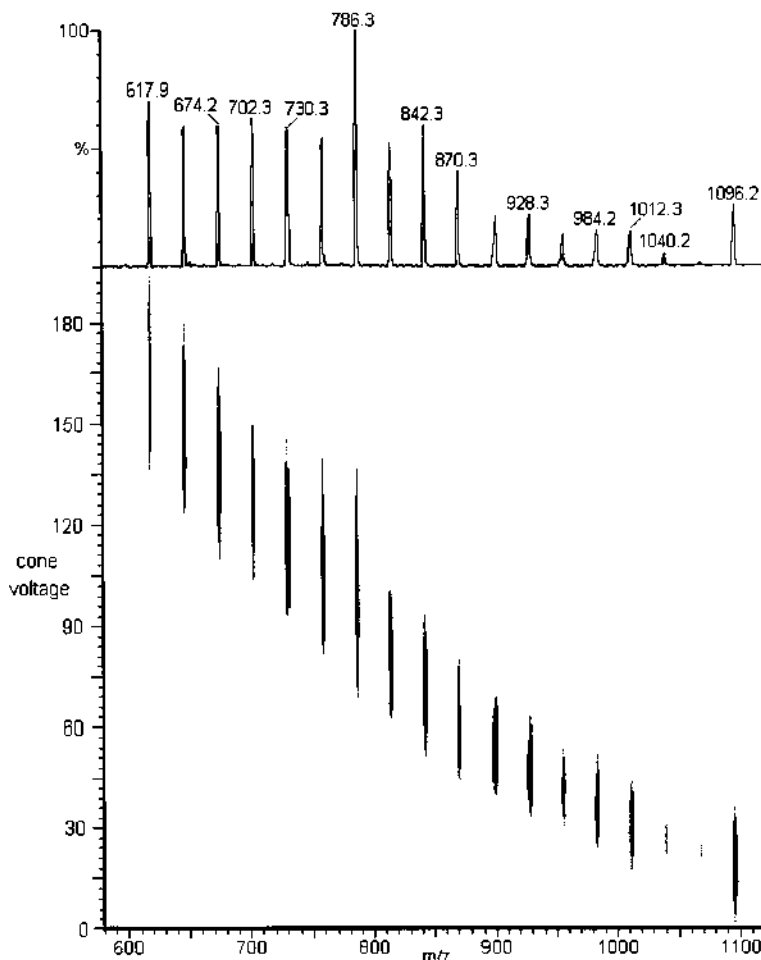


Fig. 18. An EDESI-MS two-dimensional map of m/z vs. cone voltage for $[\text{Rh}_6(\text{CO})_{16} + \text{OMe}]^-$ from 0–200 V. A combined one-dimensional spectrum appears at the top. $\text{Rh}_6(\text{CO})_{16}$ was dissolved in MeOH and derivatised in situ with a drop of $\sim 0.1 \text{ mol l}^{-1}$ solution of NaOMe in MeOH.

Because electrospray is a soft ionisation technique, very little fragmentation occurs and spectra generally consist of a single isotopomer envelope due to the parent ion. This property can be used to advantage in the study of mixtures, as each component appears in the spectrum as a single peak. For example, the pyrolysis of $\text{Os}_3(\text{CO})_{12}$ at temperatures between 210 and 260°C is known to produce a mixture of higher nuclearity osmium clusters [157]. At the lower end of this scale, the hexanuclear cluster $\text{Os}_6(\text{CO})_{18}$ is known to predominate. The crude reaction mixture from pyrolysis of $\text{Os}_3(\text{CO})_{12}$ at 210°C was dissolved, derivatised with methoxide ion and examined using ESIMS. The spectrum showed a mixture of compounds of nuclearities from four to seven, with $\text{Os}_6(\text{CO})_{18}$ the most abundant as expected.

While the lack of fragmentation observed in ESI mass spectra means that the molecular weight is easily obtained, no structural information is provided. Fragmentation can however be induced by means of increasing the cone voltage [158], which has the effect of increasing the kinetic energy of the ions in the presence of the bath gas (typically nitrogen) and fragmenting the ions by collision. In the study of clusters, this ability enables the sequential stripping of the ligands. Fig. 17 shows an example of ligand stripping for the trinuclear complex $[\text{Cr}_3\text{O}(\text{CH}_3\text{COO})_6(\text{H}_2\text{O})_3]^+$, run in a methanol mobile phase [159]. At a low cone voltages the mass spectrum shows a series of peaks corresponding to ions containing the $\text{Cr}_3\text{O}(\text{CH}_3\text{COO})_6$ core and up to three terminal ligands with various combinations of water and methanol. As the voltage is increased, collision induced decompositions occur more readily in the ion source and at a voltage of 70 V or higher, only the core ion $[\text{Cr}_3\text{O}(\text{CH}_3\text{COO})_6]^+$ has significant intensity.

A considerable amount of fragmentation data can generated in this way, and a way of presenting this data, termed 'energy-dependent electrospray ionisation mass spectrometry' (EDES-MS) is shown in Fig. 17 [160]. Fig. 18 is a two-dimensional map of mass vs. cone voltage for $[\text{Rh}_6(\text{CO})_{16} + \text{OMe}]^-$ across the entire range of cone voltages from 0–200V. At the top is a one-dimensional spectrum that combines all 201 spectra used to generate the map. This form of presentation allows assessment of the entire fragmentation pattern at a glance.

The spectrum shows the sequential loss of the ligands down to a $[\text{Rh}_6 + \text{H}]^-$ core. A loss of 30 m/z occurs midway through the fragmentation process, corresponding to a loss of H_2CO via hydride transfer from the methoxy group to the cluster. Two series of peaks are therefore seen, $[\text{Rh}_6(\text{CO})_n + \text{H}]^-$ ($n = 0-9$) at 618–870 m/z and $[\text{Rh}_6(\text{CO})_n + \text{OMe}]^-$ ($n = 9-16$) at 900–1096 m/z .

4. Summary

Cluster chemistry has benefited from the application of a wide range of increasingly powerful spectroscopic techniques to the characterisation of new compounds and studies of their reactivity. Recent advances in mass spectrometry, particularly in the area of new ionisation techniques, have also given cluster chemists new tools with which to study compounds of interest, and has allowed access to thermally unstable, involatile compounds. Spectroscopic and mass spectrometric developments have reduced the emphasis placed on X-ray crystallography for the structural characterisation of cluster compounds, and broadened the field to include the detailed study of amorphous materials, mixtures, species in solution, in the gas phase and on surfaces. As spectroscopic and mass spectrometric techniques get ever more sophisticated, thanks to innovations in instrumentation, increases in processing power, and in the development of new experimental techniques, we can safely expect their application in all areas of cluster chemistry to become more widespread.

Acknowledgements

Thanks to Professor Brian Nicholson for details of unpublished work. J.S.M. thanks the New Zealand Foundation for Research, Science and Technology for a Postdoctoral Fellowship (contract CAM801).

References

- [1] S.F.A. Kettle, E. Diana, R. Rossetti, P.L. Stanghellini, *J. Am. Chem. Soc.* 119 (1997) 8228.
- [2] S.F.A. Kettle, E. Diana, R. Rossetti, P.L. Stanghellini, *Inorg. Chem.* 37 (1998) 6502.
- [3] S.F.A. Kettle, R. Rossetti, P.L. Stanghellini, B.F.G. Johnson, *Inorg. Chim. Acta* 212 (1993) 69.
- [4] G.A. Battiston, G. Bor, U.K. Dietler, S.F.A. Kettle, R. Rossetti, G. Sbrignadello, P.L. Stanghellini, *Inorg. Chem.* 19 (1980) 1961.
- [5] S.F.A. Kettle, E. Diana, P.L. Stanghellini, R. Dellapergola, A. Fumagalli, *Inorg. Chim. Acta* 235 (1995) 407.
- [6] G. Bor, F.H. Oldani, S.F.A. Kettle, *J. Clust. Science* 9 (1998) 259.
- [7] S.F.A. Kettle, E. Diana, R. Rossetti, P.L. Stanghellini, R. Della Pergola, L. Garlaschelli, *Inorg. Chim. Acta* 227 (1994) 241.
- [8] C.E. Anson, U.A. Jayasooriya, S.F.A. Kettle, P.L. Stanghellini, R. Rossetti, *Inorg. Chem.* 30 (1991) 2282.
- [9] J.A. Creighton, R.D. Pergola, B.T. Heaton, S. Martinengo, L. Strona, D.A. Willis, *J. Chem. Soc. Chem. Commun.* (1982) 864.
- [10] J.A. Creighton, B.T. Heaton, *J. Chem. Soc. Dalton Trans.* (1981) 1498.
- [11] R.J.H. Clark, P.J. Dyson, D.G. Humphrey, B.F.G. Johnson, *Polyhedron* 17 (1998) 2985.
- [12] P. MacLaurin, N.C. Crabb, I. Wells, P.J. Worsfold, D. Coombs, *Anal. Chem.* 68 (1996) 1116.
- [13] M.J. Shaw, W.E. Geiger, *Organometallics* 15 (1996) 13.
- [14] J.M. Sanders, B.K. Hunter, *Modern NMR Spectroscopy: A Guide for Chemists*, Oxford University Press, Oxford, 1993.
- [15] W. von, E. Doering, W.R. Roth, *Angew. Chem. Int. Ed. Eng.* 2 (1963) 115.
- [16] F.A. Cotton, *Acc. Chem. Res.* 1 (1968) 257.
- [17] B.E. Mann, B.F. Taylor, *¹³C-NMR Data for Organometallic Compounds*, Academic Press, London, 1981.
- [18] D.F. Shriver, P.W. Atkins, C.H. Langford, *Inorganic Chemistry*, 2nd edition, Oxford University Press, Oxford, 1994.
- [19] J.M. Bemis, L.F. Dahl, *J. Am. Chem. Soc.* 119 (1997) 4545.
- [20] S.R. Drake, B.F.G. Johnson, J. Lewis, *J. Chem. Soc. Dalton Trans.* (1988) 1517.
- [21] P.J. Bailey, L.H. Gade, B.F.G. Johnson, J. Lewis, *Chem. Ber.* 125 (1992) 2019.
- [22] M.A. Gallop, B.F.G. Johnson, J. Keeler, J. Lewis, S.J. Hayes, C.M. Dobson, *J. Am. Chem. Soc.* 114 (1992) 2510.
- [23] F.M. Dolgushin, E.V. Grachova, B.T. Heaton, J.A. Iggo, I.O. Koshevoy, I.S. Podkorytov, D.J. Smawfield, S.P. Tunik, R. Whyman, A.I. Yanovskii, *J. Chem. Soc. Dalton Trans.* (1999) 1609.
- [24] J.L. Vidal, W.E. Walker, R.L. Pruett, R.C. Shoening, *Inorg. Chem.* 18 (1979) 129.
- [25] C. Brown, B.T. Heaton, P. Chini, A. Fumagalli, G. Longoni, *J. Chem. Soc. Chem. Commun.* (1977) 309.
- [26] C. Brown, B.T. Heaton, A.D.C. Towl, P. Chini, A. Fumagalli, G. Longoni, *J. Organomet. Chem.* 181 (1979) 233.
- [27] W. von Philipsborn, *Chem. Soc. Rev.* 28 (1999) 95 and references therein.
- [28] T. Blum, M.P. Brown, B.T. Heaton, A.S. Hor, J.A. Iggo, J.S.Z. Sabounchei, A.K.N.A. Smith, *J. Chem. Soc. Dalton Trans.* (1994) 513.
- [29] C.A. Fyfe, *Solid State NMR for Chemists*, CFC Press, Guelph, 1983.
- [30] T. Eguchi, B.T. Heaton, *J. Chem. Soc. Dalton Trans.* (1999) 3523.

- [31] S. Aime, W. Dastru, R. Gobetto, A.J. Arce, *Organometallics* 13 (1994) 4232.
- [32] M.A. Gallop, B.F.G. Johnson, J. Lewis, P.R. Raithby, *J. Chem. Soc. Chem. Commun.* (1987) 1809.
- [33] P. Kempgens, J. Hirschinger, K. Elbayed, J. Raya, P. Granger, J. Rose, *J. Phys. Chem.* 100 (1996) 2045.
- [34] J.V. Barkley, T. Eguchi, R.A. Harding, B.T. Heaton, G. Longoni, L. Manzi, H. Nakayama, K. Miyagi, A.K. Smith, A. Steiner, *J. Organomet. Chem.* 573 (1999) 254.
- [35] L.J. Farrugia, D. Braga, F. Grepioni, *J. Organomet. Chem.* 573 (1999) 60.
- [36] K.Y. Yang, S.G. Bott, M.G. Richmond, *Organometallics* 14 (1995) 2718.
- [37] J.P. Scott, J.R. Budge, A.L. Rheingold, B.C. Gates, *J. Am. Chem. Soc.* 109 (1987) 7736.
- [38] J.G.C. Shen, A.M. Liu, T. Tanaka, M. Ichikawa, *J. Phys. Chem. B* 102 (1998) 7782.
- [39] M.P. Cifuentes, M.G. Humphrey, G.A. Heath, *Inorg. Chim. Acta* 259 (1997) 273.
- [40] A. Vértes, L. Korecz, K. Burger, *Mössbauer Spectroscopy*, Elsevier, Amsterdam, 1979.
- [41] R.H. Herber, W.R. Kingston, G.K. Wertheim, *Inorg. Chem.* 2 (1963) 153.
- [42] G. Schmid, *Struct. Bonding* 62 (1985) 52.
- [43] K. Burger, L. Korecz, G. Bor, *J. Inorg. Nucl. Chem.* 31 (1969) 1527.
- [44] R. Reina, O. Rossell, M. Seco, P. GomezSal, A. Martin, D. deMontauzon, A. Mari, *Organometallics* 17 (1998) 4127.
- [45] Y. Iwasawa, *X-Ray Absorption Fine Structure for Catalysts and Surfaces*, World Scientific, Singapore, 1996.
- [46] J.G.C. Shen, M. Ichikawa, *J. Phys. Chem. B* 102 (1998) 5602.
- [47] W.A. Weber, B.C. Gates, *J. Catal.* 180 (1998) 207.
- [48] J.G.C. Shen, A.M. Liu, M. Ichikawa, *J. Chem. Soc. Faraday Trans.* 94 (1998) 1353.
- [49] G.J. Liu, T. Fujimoto, A. Fukuoka, M. Ichikawa, *Catal. Lett.* 12 (1992) 171.
- [50] W. Vogel, H. Knozinger, B.T. Carvill, W.M.H. Sachtler, Z.C. Zhang, *J. Phys. Chem. B* 102 (1998) 1750.
- [51] M.S. Nashner, A.I. Frenkel, D.L. Adler, J.R. Shapley, R.G. Nuzzo, *J. Am. Chem. Soc.* 119 (1997) 7760.
- [52] K. Okumura, K. Asakura, Y. Iwasawa, *J. Phys. Chem. B* 101 (1997) 9984.
- [53] R. Raja, G. Sankar, S. Hermans, D.S. Shephard, S. Bromley, J.M. Thomas, B.F.G. Johnson, *Chem. Commun.* (1999) 1571.
- [54] S.E. Deutsch, G. Mestl, H. Knozinger, B.C. Gates, *J. Phys. Chem. B* 101 (1997) 1374.
- [55] S.P. Gubin, T.V. Galuzina, I.F. Golovaneva, A.P. Klyagina, L.A. Polyakova, O.A. Belyakova, Y.V. Zubavichus, Y.L. Slovokhotov, *J. Organomet. Chem.* 549 (1997) 55.
- [56] I.I. Moiseev, *J. Organomet. Chem.* 488 (1995) 183.
- [57] D. Ellis, L.J. Farrugia, P. Wiegeleben, J.G. Crossley, A.G. Orpen, P.N. Waller, *Organometallics* 14 (1995) 481.
- [58] A.J. Dent, L.J. Farrugia, A.G. Orpen, S.E. Stratford, *J. Chem. Soc. Chem. Commun.* (1992) 1456.
- [59] L.J. Farrugia, N. Macdonald, R.D. Peacock, *J. Chem. Soc. Chem. Commun.* (1991) 163.
- [60] M.C.R. Symons, *Chemical and Biochemical Aspects of Electron-Spin Resonance*, Wiley, New York, 1978.
- [61] A. Bencini, D. Gatteschi, in: E.I. Solomon, A.B.P. Lever (Eds.), *Inorganic Electronic Structure and Spectroscopy*, Wiley, New York, 1999.
- [62] F. Calderoni, F. Demartin, M.C. Iapalucci, F. Laschi, G. Longoni, P. Zanello, *Inorg. Chem.* 35 (1996) 898.
- [63] D.S. Shephard, B.F.G. Johnson, A. Harrison, S. Parsons, S.P. Smidt, L.J. Yellowlees, *J. Organomet. Chem.* 563 (1998) 113.
- [64] D.A. Nagaki, J.V. Badding, A.M. Stacy, L.F. Dahl, *J. Am. Chem. Soc.* 108 (1986) 3825.
- [65] V.G. Albano, L. Grossi, G. Longoni, M. Monari, S. Mulley, A. Sironi, *J. Am. Chem. Soc.* 114 (1992) 5708.
- [66] R.B. King, *Inorg. Chim. Acta* 227 (1994) 207.
- [67] J.J. Thomson, *Rays of Positive Electricity and their Application to Chemical Analysis*, Longmans, Green & Co, London, 1913.

- [68] M. Tsutsui, *Characterization of Organometallic Compounds, Part I*, Interscience, New York, 1969.
- [69] D.T. Hurd, G.W. Sentell, F.G. Norton, *J. Am. Chem. Soc.* 71 (1949) 1899.
- [70] R.E. Winters, R.W. Kiser, *J. Phys. Chem.* 69 (1965) 1618.
- [71] R.B. King, *J. Am. Chem. Soc.* 88 (1966) 2075.
- [72] B.F.G. Johnson, J. Lewis, I.G. Williams, J.M. Wilson, *J. Chem. Soc. (A)* (1967) 341.
- [73] W. Fellman, D.K. Huggins, H.D. Kaesz, J.M. Smith, *J. Am. Chem. Soc.* 86 (1964) 4841.
- [74] B.F.G. Johnson, R.D. Johnston, J. Lewis, B.H. Robinson, *J. Chem. Soc. Chem. Commun.* (1966) 851.
- [75] M.T. Bowers, A.G. Marshall, F.W. McLafferty, *J. Phys. Chem.* 100 (1996) 12897.
- [76] M.S.B. Munson, F.H. Field, *J. Am. Chem. Soc.* 88 (1966) 2621.
- [77] M.S.B. Munson, *Anal. Chem.* 43 (1971) 28A.
- [78] C.R. Eady, B.F.G. Johnson, J. Lewis, *J. Chem. Soc. Dalton Trans.* (1975) 2606.
- [79] A.G. Marshall, *Acc. Chem. Res.* 18 (1985) 316.
- [80] S.G. Shore, D.-Y. Jan, W.-L. Hsu, L.-Y. Hsu, S. Kennedy, J.C. Huffman, T.-C. Lin Wang, A.G. Marshall, *J. Chem. Soc. Chem. Commun.* (1984) 392.
- [81] L.-Y. Hsu, W.-L. Hsu, D.-Y. Jan, A.G. Marshall, S.G. Shore, *Organometallics* 3 (1984) 591.
- [82] C.L. Hammill III, R.J. Clark, C.W. Ross, A.G. Marshall, J. Schmutz, *Inorg. Chem.* 36 (1997) 5973.
- [83] W.K. Meckstroth, R.B. Freas, W.D. Reents Jr., D.P. Ridge, *Inorg. Chem.* 24 (1985) 3139.
- [84] S.L. Mullen, A.G. Marshall, *J. Am. Chem. Soc.* 110 (1988) 1766.
- [85] D.L. Vollmer, M.L. Gross, R.J. Waugh, M.I. Bruce, J.H. Bowie, *Organometallics* 13 (1994) 3564.
- [86] R.S. Houk, *Acc. Chem. Res.* 27 (1994) 33.
- [87] T.G.M.M. Kappen, P.P.J. Schlebos, J.J. Bour, W.P. Bosman, J.M.M. Smits, P.T. Beurskens, J.J. Steggerda, *J. Am. Chem. Soc.* 117 (1995) 8327.
- [88] T.G.M.M. Kappen, P.P.J. Schlebos, J.J. Bour, W.P. Bosman, J.M.M. Smits, P.T. Beurskens, J.J. Steggerda, *Inorg. Chem.* 34 (1995) 2133.
- [89] D.M. Sellsell, A.G. Sykes, *Inorg. Chem.* 35 (1996) 5536.
- [90] R. Hernandez-Molina, D.N. Dybtsev, V.P. Fedin, M.R.J. Elsegood, W. Clegg, A.G. Sykes, *Inorg. Chem.* 37 (1998) 2995.
- [91] W.D. Reynolds, *Anal. Chem.* 51 (1979) 283A.
- [92] W.P. Mul, C.J. Elsevier, M. Vanleijen, K. Vrieze, W.J.J. Smeets, A.L. Spek, *Organometallics* 11 (1992) 1877.
- [93] O.C.P. Beers, C.J. Elsevier, W.J.J. Smeets, A.L. Spek, *Organometallics* 12 (1993) 3199.
- [94] R.J. Beuhler, E. Flanigan, L.J. Green, L. Friedman, *J. Am. Chem. Soc.* 96 (1974) 3990.
- [95] D.A. Morgenstern, C.C. Bonham, A.P. Rothwell, K.V. Wood, C.P. Kubiak, *Polyhedron* 14 (1995) 1129.
- [96] J.M. Hughes, Y. Huang, R.D. MacFarlane, C.J. McNeal, G.J. Lewis, L.F. Dahl, *Int. J. Mass Spec. Ion Process.* 126 (1993) 197.
- [97] C.J. McNeal, J.M. Hughes, G.J. Lewis, L.F. Dahl, *J. Am. Chem. Soc.* 113 (1991) 372.
- [98] C.J. McNeal, R.E.P. Winpenny, R.D. MacFarlane, L.H. Pignolet, L.T.J. Nelson, T.G. Gardner, L.H. Irgens, G. Vigh, J.P. Fackler, *Inorg. Chem.* 32 (1993) 5582.
- [99] J.P. Fackler, C.J. McNeal, L.H. Pignolet, R.E.P. Winpenny, *J. Am. Chem. Soc.* 111 (1989) 6434.
- [100] G. Schmid, *Chem. Rev.* 92 (1992) 1709 and references therein.
- [101] M. Barber, R.S. Bordoli, R.D. Sedgwick, A.N. Tyler, *J. Chem. Soc. Chem. Commun.* (1981) 325.
- [102] C. Fenselau, R.J. Cotter, *Chem. Rev.* 87 (1987) 501.
- [103] T.J. Kamp, *Coord. Chem. Rev.* 125 (1993) 333.
- [104] J.L. Haggitt, D.M.P. Mingos, *J. Chem. Soc. Dalton Trans.* (1994) 1013.
- [105] K. Lee, J.R. Shapley, *Organometallics* 17 (1998) 4368.
- [106] L.Q. Ma, U. Brand, J.R. Shapley, *Inorg. Chem.* 37 (1998) 3060.
- [107] P.D. Boyle, B.J. Johnson, B.D. Alexander, J.A. Casalnuovo, P.R. Gannon, S.M. Johnson, E.A. Larka, A.M. Muetting, L.H. Pignolet, *Inorg. Chem.* 26 (1987) 1346.
- [108] R.C.B. Copley, D.M.P. Mingos, *J. Chem. Soc. Dalton Trans.* (1996) 491.
- [109] T. Chihara, L.P. Yang, Y. Esumi, Y. Wakatsuki, *J. Mass Spec.* 30 (1995) 684.

- [110] S.M. Malinak, L.K. Madden, H.A. Bullen, J.J. McLeod, D.C. Gaswick, *Inorg. Chim. Acta* 278 (1998) 241.
- [111] F. Hillenkamp, M. Karas, R.C. Beavis, B.T. Chait, *Anal. Chem.* 63 (1991) 1193.
- [112] M. Karas, U. Bahr, A. Ingendoh, F. Hillenkamp, *Angew. Chem. Int. Ed. Engl.* 28 (1989) 760.
- [113] D.C. Muddiman, R. Bakhtiar, S.A. Hofstadler, R.D. Smith, *J. Chem. Educ.* 74 (1997) 1288.
- [114] M.J. Dale, P.J. Dyson, B.F.G. Johnson, P.R.R. Langridge-Smith, H.T. Yates, *J. Chem. Soc. Chem. Commun.* (1995) 1689.
- [115] M.J. Dale, P.J. Dyson, B.F.G. Johnson, C.M. Martin, P.R.R. Langridge-Smith, R. Zenobi, *J. Chem. Soc. Dalton Trans.* (1996) 771.
- [116] G. Critchley, P.J. Dyson, P.R.R. Langridge-Smith, B.F.G. Johnson, J.S. McIndoe, R.K. O'Reilly, *Organometallics* 18 (1999) 4090.
- [117] P.J. Dyson, A.K. Hearley, B.F.G. Johnson, J.S. McIndoe, P.R.R. Langridge-Smith, *Inorg. Chem. Commun.* 2 (1999) 590.
- [118] P.J. Dyson, P.R.R. Langridge-Smith, B.F.G. Johnson, J.S. McIndoe, unpublished results.
- [119] M.E. Barr, B.R. Adams, R.R. Weller, L.F. Dahl, *J. Am. Chem. Soc.* 113 (1991) 3052.
- [120] A. Bjarnason, R.E. Desenfans, M.E. Barr, L.F. Dahl, *Organometallics* 9 (1990) 657.
- [121] S. Martinovic, L.P. Tolic, D. Szic, N. Kezele, D. Plavsic, L. Klasinc, *Rapid Commun. Mass Spectrom.* 10 (1996) 51.
- [122] N.C. Dopke, P.M. Treichel, M.M. Vestling, *Inorg. Chem.* 37 (1998) 1272.
- [123] R.W. McGaff, R.K. Hayashi, D.R. Powell, P.M. Treichel, *Polyhedron* 17 (1998) 4425.
- [124] C. Kim, I. Jung, *Inorg. Chem. Commun.* 1 (1998) 427.
- [125] C. Kim, I. Jung, *J. Organomet. Chem.* 588 (1999) 9.
- [126] J.H. Elnakat, K.J. Fisher, I.G. Dance, G.D. Willett, *Inorg. Chem.* 32 (1993) 1931.
- [127] J.H. Elnakat, I.G. Dance, K.J. Fisher, D. Rice, G.D. Willett, *J. Am. Chem. Soc.* 113 (1991) 5141.
- [128] I.G. Dance, K.J. Fisher, G.D. Willett, *J. Chem. Soc. Dalton Trans.* (1997) 2557.
- [129] S.A. Hofstadler, R. Bakhtiar, R.D. Smith, *J. Chem. Educ.* 73 (1996) A82.
- [130] M. Dole, L.L. Mack, R.L. Hines, R.C. Mobley, L.D. Fergusson, M. Alice, *J. Chem. Phys.* 49 (1968) 2240.
- [131] J.B. Fenn, M. Mann, C.K. Meng, S.F. Wong, C.M. Whitehouse, *Mass Spectrosc. Rev.* 9 (1990) 37.
- [132] J.B. Fenn, M. Mann, C.K. Meng, S.F. Wong, C.M. Whitehouse, *Science* 246 (1989) 64.
- [133] I. Jardine, *Nature* 345 (1990) 747.
- [134] M. Yamashita, J.B. Fenn, *J. Phys. Chem.* 88 (1984) 4451.
- [135] R. Colton, A. D'Agostino, J.C. Traeger, *Mass Spectrosc. Rev.* 14 (1995) 79.
- [136] V. Katta, S.K. Chowdbury, B.T. Chait, *J. Am. Chem. Soc.* 112 (1990) 319.
- [137] R. Colton, J.C. Traeger, *Inorg. Chim. Acta* 201 (1992) 153.
- [138] D.K. Walanda, R.C. Burns, G.A. Lawrance, E.I. von Nagy-Felsobuki, *J. Chem. Soc. Dalton Trans.* (1999) 311.
- [139] W. Henderson, B.K. Nicholson, L.J. McCaffrey, *Polyhedron* 17 (1998) 4291.
- [140] M. Ferrer, R. Reina, O. Rossell, M. Seco, G. Segalés, *J. Organomet. Chem.* 515 (1996) 205.
- [141] R. Reina, O. Riba, O. Rossell, M. Seco, P. Gómez-Sal, A. Martín, *Organometallics* 16 (1997) 5113.
- [142] P.D. Mlynek, L.F. Dahl, *Organometallics* 16 (1997) 1655.
- [143] W. Henderson, J.S. McIndoe, B.K. Nicholson, P.J. Dyson, *J. Chem. Soc. Dalton Trans.* (1998) 519.
- [144] D.J.F. Bryce, P.J. Dyson, B.K. Nicholson, D.G. Parker, *Polyhedron* 17 (1998) 2899.
- [145] Y.Y. Choi, W.-T. Wong, *J. Chem. Soc. Dalton Trans.* (1999) 331.
- [146] A.M. Bond, R. Colton, J.C. Traeger, J. Harvey, *Inorg. Chim. Acta* 212 (1993) 233.
- [147] R.A. Croft, D.N. Duffy, B.K. Nicholson, *J. Chem. Soc. Dalton Trans.* (1982) 1023.
- [148] D.N. Duffy, K.M. Mackay, B.K. Nicholson, R.A. Thomson, *J. Chem. Soc. Dalton Trans.* (1982) 1029.
- [149] C.E. Evans, B.K. Nicholson, Personal communication.
- [150] B.K. Nicholson, Personal communication.

- [151] W. Henderson, J.S. McIndoe, B.K. Nicholson, P.J. Dyson, *J. Chem. Soc. Chem. Commun.* (1996) 1183.
- [152] J.S. McIndoe, B.K. Nicholson, *J. Organomet. Chem.* 573 (1999) 232.
- [153] W. Henderson, B.K. Nicholson, *J. Chem. Soc. Chem. Commun.* (1995) 2531.
- [154] H. Hori, J. Ishihara, K. Koike, K. Takeuchi, T. Ibusuki, O. Ishitani, *Chem. Lett.* (1997) 273.
- [155] S. Chand, R.K. Coll, J.S. McIndoe, *Polyhedron* 17 (1998) 507.
- [156] C. Decker, W. Henderson, B.K. Nicholson, *J. Chem. Soc. Dalton Trans.* (1999) 3507.
- [157] J.N. Nichols, M.D. Vargas, *Inorg. Synth.* 28 (1990) 289.
- [158] L.A.P. Kane-Maguire, R. Kanitz, M.M. Sheil, *J. Organomet. Chem.* 486 (1995) 243.
- [159] A. van den Bergen, R. Colton, M. Percy, B.O. West, *Inorg. Chem.* 32 (1993) 3408.
- [160] P.J. Dyson, B.F.G. Johnson, J.S. McIndoe, P.R.R. Langridge-Smith, *Rapid Commun. Mass Spectrom.* 14 (2000) 311.